Photosynthesis Research **31**: 167–194, 1992.

Minireview

Applications of spectral hole burning spectroscopies to antenna and reaction center complexes

N. Raja S. Reddy, Paul A. Lyle* & Gerald J. Small
Ames Laboratory-USDOE and Department of Chemistry, Iowa State University, Ames, IA 50011, USA

Received 18 June 1991; accepted in revised form 27 September 1991

Key words: energy transfer, Photosystem I, II, *Rhodobacter sphaeroides*, *Prosthecochloris aestuarii*

Abstract

The underlying principles of spectral hole burning spectroscopies and the theory for hole profiles are reviewed and illustrated with calculated spectra. The methodology by which the dependence of the overall hole profile on burn wavelength can be used to reveal the contributions from site inhomogeneous broadening and various homogeneous broadening contributions to the broad Q_y-absorption bands of cofactors is emphasized. Applications to the primary electron donor states of the reaction centers of purple bacteria and Photosystems I and II of green plants are discussed. The antenna (light harvesting) complexes considered include B800–B850 and B875 of *Rhodobacter sphaeroides* and the base-plate complex of *Prosthecochloris aestuarii* with particular attention being given to excitonic interactions and level structure. The data presented show that spectral hole burning is a generally applicable low temperature approach for the study of excited state electronic and vibrational (intramolecular, phonon) structures, structural heterogeneity and excited state lifetimes.

I. Introduction

Extensive theoretical and experimental investigations have been performed on the primary optical excitation (energy) transfer (Pearlstein 1982, van Grondelle 1985, Knox 1986, Hunter et al. 1989) and charge separation events (Kirmaier et al. 1987, Friesner et al. 1989b, Norris et al. 1990) of photosynthesis. Each represents a formidable problem for any protein-pigment complex even when an X-ray structure is available. For example, a definitive explanation of primary charge separation in bacterial reaction centers (RC) is wanting even though the structure of the RC of *Rhodopseudomonas viridis* has been known for eight years (Deisenhofer et al. 1984). Also, the circular dichroism spectra of the base-plate antenna complex of the green algae *Prosthecochloris aestuarii* have defied interpretation since its structure was determined in 1979. This complex is an important test case for theory because of the existence of strong excitonic interactions between bacteriochlorophylls (BChl) (Mathews et al. 1979). For these and other systems, time and conventional frequency domain data have been invaluable for the testing and development of theoretical models. These data sometimes appear to present a paradox. For example, the linear dichroism spectra of bacterial RC indicate that, aside from a strong excitonic interaction within the special pair, the accessory BChl and BPheo (bacteriopheophytin) molecules behave like weakly coupled chromophores which is inconsistent with the finding that the Q_y-states of the accessory pigments undergo downward energy transfer in <100 fs (Breton et al. 1988a, John-

* William E. Catron Fellow.

son et al. 1990). The primary charge separation kinetics for the RC of Photosystem II (PS II), including its temperature dependence (Johnson et al. 1989b, Wasielewski et al. 1989a, 1989b), are very similar to those of bacterial RC and yet, energy transfer from the Q_y-states of the accessory chlorophylls (Chl) and active pheophytin (Pheo) is over two orders of magnitude slower than in bacterial RC (Tang et al. 1990a, 1990c). It is important to explain primary charge separation and energy transfer processes in RC in a self-consistent manner since they are both linked to the excited state electronic-vibrational structures of the coupled chromophore system. Other factors which need to be considered, especially since the temperature dependences of transport processes have been used to provide further insight into the dynamics, are structural heterogeneity (from complex to complex), which leads to a distribution of values for the relevant energy gap(s) in the transport process, and the homogeneous broadenings of the states involved.

Spectral hole burning spectroscopies have provided the first information on heterogeneity (site inhomogeneous band broadening) and homogeneous broadening of excited states of photosynthetic units due, for example, to linear electron-phonon coupling (i.e., optical reorganization energies have now been measured) and exciton level structure and inter-exciton level scattering. Furthermore, spectral hole burning has been used to test some of the basic assumptions of non-adiabatic transport theories and yielded the kinetics of ultra-fast processes which would be difficult to obtain in the time domain.

Prior to their application to photosynthetic complexes, non-photochemical and photochemical hole burning (NPHB, PHB) and triplet population bottleneck hole burning spectroscopies were applied to chromophores imbedded in organic glasses and synthetic polymers. The lowest $^1\pi\pi^*$ states of aromatic molecules and laser dyes have been most extensively studied. Several review articles (Freidrich et al. 1984, Jankowiak et al. 1987b, Volker 1989, Narasimhan et al. 1990) and, very recently, a book (Moerner 1987) have been written on the principles of solid state hole-burning spectroscopies and their application to several problems including the pure dephasing of optical transitions and dispersive kinetics in glasses at low temperatures.

Hole burning has led to an improvement in the resolution of the optical absorption spectra of Chl and Pheo molecules of protein complexes of up to 4 orders of magnitude. This results from the elimination of the contribution from site inhomogeneity (Γ_I) to the absorption bandwidths. It is now routinely possible to 'get under the skin' of broad ($\sim$100–500 cm^{-1}) cofactor absorption bands to determine both Γ_I and the homogeneous broadening contribution (Γ_H) to the bandwidth. There are several Γ_H-mechanisms which can be important for the dynamics of the primary events. Hole burning can also be used to resolve closely spaced electronic states in complexes and to generate a high level of detail on excited state intramolecular vibrational frequencies and Franck–Condon factors.

The organization of this article is as follows: First, the principles of hole burning spectroscopies are discussed with particular attention being paid to the nature of the low temperature absorption spectrum of a *single* chromophore in a matrix and how this spectrum, together with intrinsic disorder, leads to the observed absorption spectrum. Also discussed is a theory for spectral hole profiles which depend on the location of the burn frequency within the absorption band. This section is followed by two which deal with recent applications of hole burning to the primary electron donor state (P*) of RC and light harvesting complexes (LHC). Since a review, based on work published up to the middle of 1989, has just appeared (Johnson et al. 1991b), no attempt is made here to review holeburning studies reported prior to that time except when they are relevant to the new results discussed. We present some unpublished data on the fully deuterated RC of wild type *Rhodobacter sphaeroides* (*Rb. sphaeroides*) and on the CP47–D1–D2 complex of PS II. In so doing we ask a number of questions, two of which are whether deuteration has any effect on the underlying structure of P870 (absorption band of ground state P or special pair) and the lifetime of P* and whether the underlying structures of P870 (or P960 of *Rhodopseudomonas viridis*, *Rps. viridis*) differ from P680 (the primary ground state absorption of PS II) and what the hole burned spectra say about P680 being due to a special pair. Hole burning is the only existing technique for measuring the lifetime of P* for a well-

defined phononic-vibronic level, the total zero-point level. A not unimportant question is whether or not the time and frequency domain experiments yield the same lifetime for P* since it speaks to the question of whether thermalization of low frequency intermolecular modes precedes primary charge separation (non-adiabatic electron-transfer theories, as practiced, assume that it does). There is also the question of whether P* undergoes ultra-fast ($\leqslant$100 fs (Won et al. 1988a, 1988b, 1987, Friesner et al. 1989a)) electronic relaxation prior to formation of the primary charge-separated state of the RC (e.g., P^+BPheo^- of bacterial RC). The section on RC is followed by one that discusses the temperature dependence of energy transfer in the antenna complex of *Rb. sphaeroides* and describes a novel approach for the determination of the 'exciton bandwidth' of chromophore aggregates. Finally, data are presented which speak to excitonic interactions and inter-exciton level scattering in the base-plate antenna complex of *P. aestuarii*.

For the convenience of the reader a glossary of the less familiar terms used in the text is included as an appendix.

II. Principles and theory of solid state spectral hole burning

In condensed phase systems there are several mechanisms by which optical transitions and spectra are broadened. All can be categorized, however, as homogeneous or inhomogeneous. Often the two are defined and contrasted in terms of a single well defined transition. Homogeneous broadening is that which is the same for each and every chemically identical molecule in the ensemble. In the gas phase one could consider, for example, absorption from the rotationless and vibrationless (zero-point level) of the ground electronic state to a particular rotational-vibrational level of an electronically excited state. At sufficiently low pressure this rovibronic transition would be homogeneously broadened due to the finite lifetime (τ_1) of the excited state with a full width half-maximum (i.e., FWHM (cm^{-1}) = $(2\pi c\tau_1)^{-1}$) where c is the speed of light. For $\tau_1 = 5$ ns, FWHM $\approx$ 0.001 cm^{-1}. At room temperature this lifetime broadening is negligible compared to the Doppler broadening, which is a manifestation of the distribution of molecular velocities which leads to a Gaussian distribution of transition frequencies. This 'heterogeneity' in frequencies is an example of inhomogeneous line broadening.

The solid state analog of rotational structure is phonon (lattice-vibrational) sideband structure; it is a manifestation of the change in the lattice equilibrium structure which accompanies the electronic excitation. The analog of Doppler broadening is site inhomogeneous broadening, which is the result of an analyte or probe molecule in a solid host adopting energetically inequivalent sites. This leads to a Gaussian distribution of frequencies for any given vibronic transition. For amorphous hosts, such as glasses and polymers, the inhomogeneous broadening, Γ_I, is 100–300 cm^{-1}.

A. Principles

Figure 1 depicts an inhomogeneously broadened origin or vibronic absorption band at low temperature. The sharp dashed bands are the zero-phonon lines (ZPL) of the 'guest' molecule occupying inequivalent sites. A zero-phonon transition is one for which no net change in the number of phonons accompanies the electronic transition. Building to higher energy on each ZPL is a broad phonon (lattice vibrational) wing or phonon sideband (PSB). Each single site ZPL carries a homogeneous linewidth, γ, which is determined by the total dephasing time τ_2 of the optical transition:

$$\frac{1}{\tau_2} = \frac{1}{2\tau_1} + \frac{1}{\tau_2'} \tag{1}$$

where τ_1 is the excited state lifetime and τ_2' is the pure dephasing time. The latter is best understood in terms of the density matrix formulation of spectroscopic transitions (Sargeant et al. 1974, Levenson et al. 1982). For our purposes it suffices to say that τ_2' is due to the modulation of the single site transition frequency which results from the interaction of the excited state with the bath phonons (and other low energy excitations in glasses (Hayes et al. 1987)). This interaction does not lead to electronic relaxation of the excited state but rather to a decay of the phase

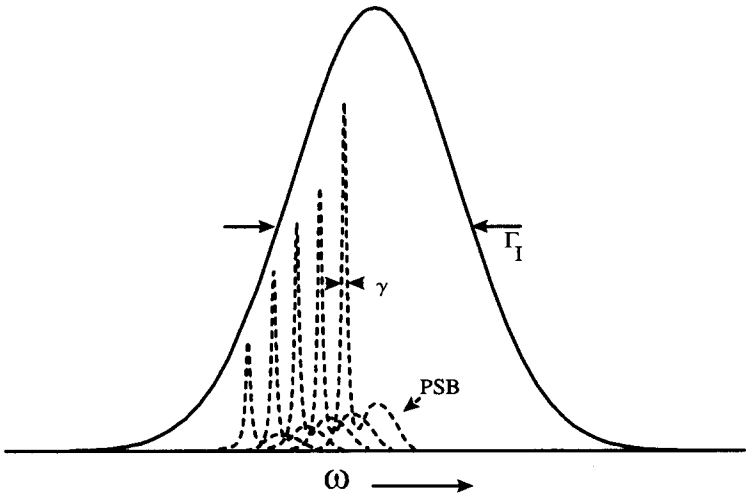

Fig. 1. Schematic representation of homogeneous (γ) and inhomogeneous (Γ_I) broadening. Profiles of the zero-phonon lines (ZPL) and their associated side bands (PSB) for specific sites at different frequencies have been enlarged compared to the inhomogeneous line to provide more detail.

coherence of the superposition state initially created by the photon (Levenson et al. 1988). In units of cm^{-1}, $\gamma = (\pi\tau_2 c)^{-1}$ where c is the speed of light in $cm\,s^{-1}$.

γ determines the ultimate spectral resolution attainable by line narrowing techniques. A key point is that τ_2' is strongly temperature dependent. Pure dephasing theories are now well developed (Huber et al. 1984, Lyo 1986, Hayes et al. 1987) and photon echo (Narasimhan et al. 1990) and spectral hole burning (Walsh et al. 1986, Haarer 1987, Hayes et al. 1987, Jankowiak et al. 1987b, Walsh et al. 1987b, Berg et al. 1988, Volker 1989) have been used to study the temperature dependence of τ_2' in a wide variety of glassy systems. At room temperature, γ from τ_2' is $\approx kT$, i.e., $\approx 200\,cm^{-1}$, which is comparable to Γ_I for glasses. Line narrowing spectroscopies cannot eliminate γ, which means that low temperatures are required to minimize the number of thermally populated low frequency phonon and other excitations responsible for γ. For glass hosts it is now firmly established that γ from pure dephasing and/or spectral diffusion is $\leq 0.1\,cm^{-1}$ at 4.2 K, which is negligible relative to $\gamma = 5\,cm^{-1}$ from $\tau_1 = 1$ ps. Spectral diffusion describes the broadening of the absorption line due to fluctuations in glass host on a time scale longer than the excited state lifetime.

Three types of hole burning spectroscopy have been applied to protein-pigment complexes: non-photochemical (NPHB), photochemical (PHB) and triplet population bottleneck. With an understanding of site inhomogeneous broadening and isochromat selection by a narrow line laser, PHB follows in a natural way. What is required is that the absorbing chromophore be photoreactive. Only the ZPL of sites contributing to absorption at ω_L will be excited. As a consequence, isochromat selective photobleaching occurs and a zero-phonon hole (ZPH) will appear at ω_L, see the ZPH at ω_L in the Δ-absorbance spectrum of Fig. 2A. Provided the photochemistry is irreversible, photochemical holes are persistent provided the sample is held at a low temperature. Photoreactivity is not required in NPHB. However, NPHB is generally observed only for glassy hosts. A mechanistic model for persistent NPHB was first proposed in 1978 (Hayes et al. 1978) and recently has been improved upon (Shu et al. 1990). Both, however, are based on the inherent structural disorder of a glass and phonon-assisted tunneling between different impurity-glass configurations. In simplest terms: upon completion of the ground state → excited state → ground state cycle, the host configuration around the impurity is altered, more or less permanently; the change in environment produces a shift of the ZPL frequency at ω_L to other regions of the inhomogeneously broadened absorption profile. This leads to increased absorption at frequencies other than ω_L (antihole).

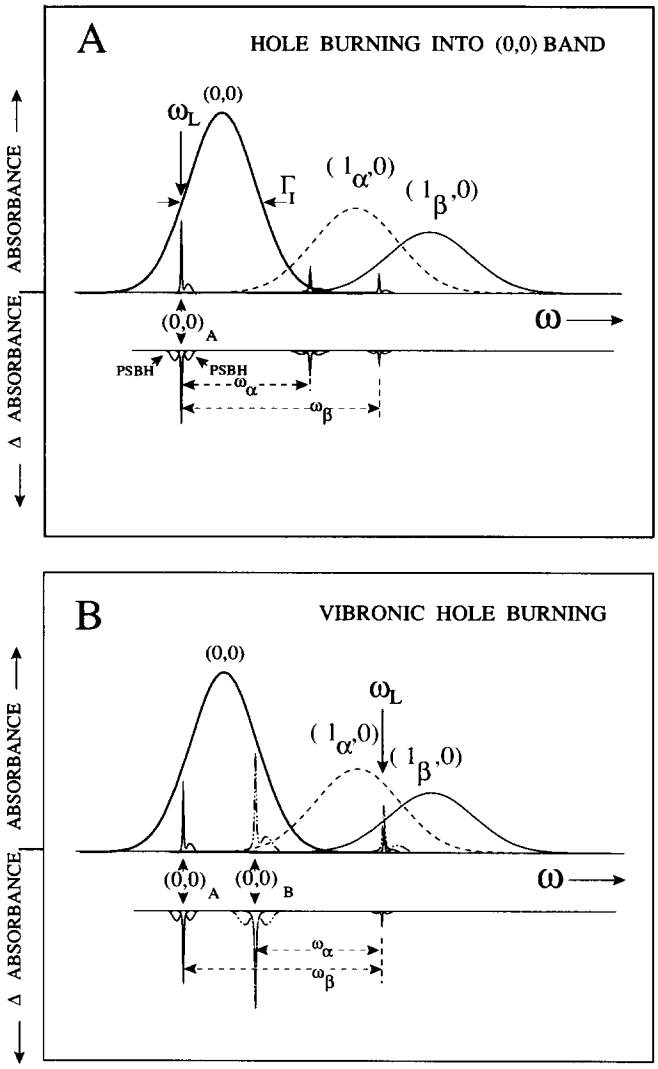

Fig. 2. Schematic of hole burning (selective photobleaching) into origin band (A) and into vibronic region (B).

In the absorbance spectrum of Fig. 2A the burn frequency excites an isochromat in the (0, 0) or origin band. However, the sites that contribute to the origin isochromat also contribute to the $(1_\alpha, 0)$ and $(1_\beta, 0)$ vibronic bands. Thus, a ZPH burnt at ω_L can be accompanied by higher energy vibronic satellite holes. Because the ZPL is accompanied by a PSB, the ZPH is accompanied by phonon sideband holes (PSBH). The PSBH to higher energy of the ZPH is readily understood and is referred to as the real-PSBH. The pseudo-PSBH is due to sites whose ZPL frequencies lie to lower energy of ω_L and which absorb the laser light by virtue of the PSB. The phonons excited rapidly relax to the zero-point level after which hole burning ensues. A recent example of persistent ZPH and PSBH structure for the isolated reaction center complex of PS II at 4.2 K is shown in Fig. 3B. The hole structure is due to the Q_y-state of the Pheo *a* molecule active in primary charge separation (Tang et al. 1990a, Tang et al. 1990c).

In the same manner that the pseudo-PSBH can be produced, pseudo-vibronic hole structure can be generated. In Fig. 2B the burn frequency (ω_L) excites isochromats belonging to vibrations α and β. Since the time constant for hole burning is long relative to the vibrational relaxation time,

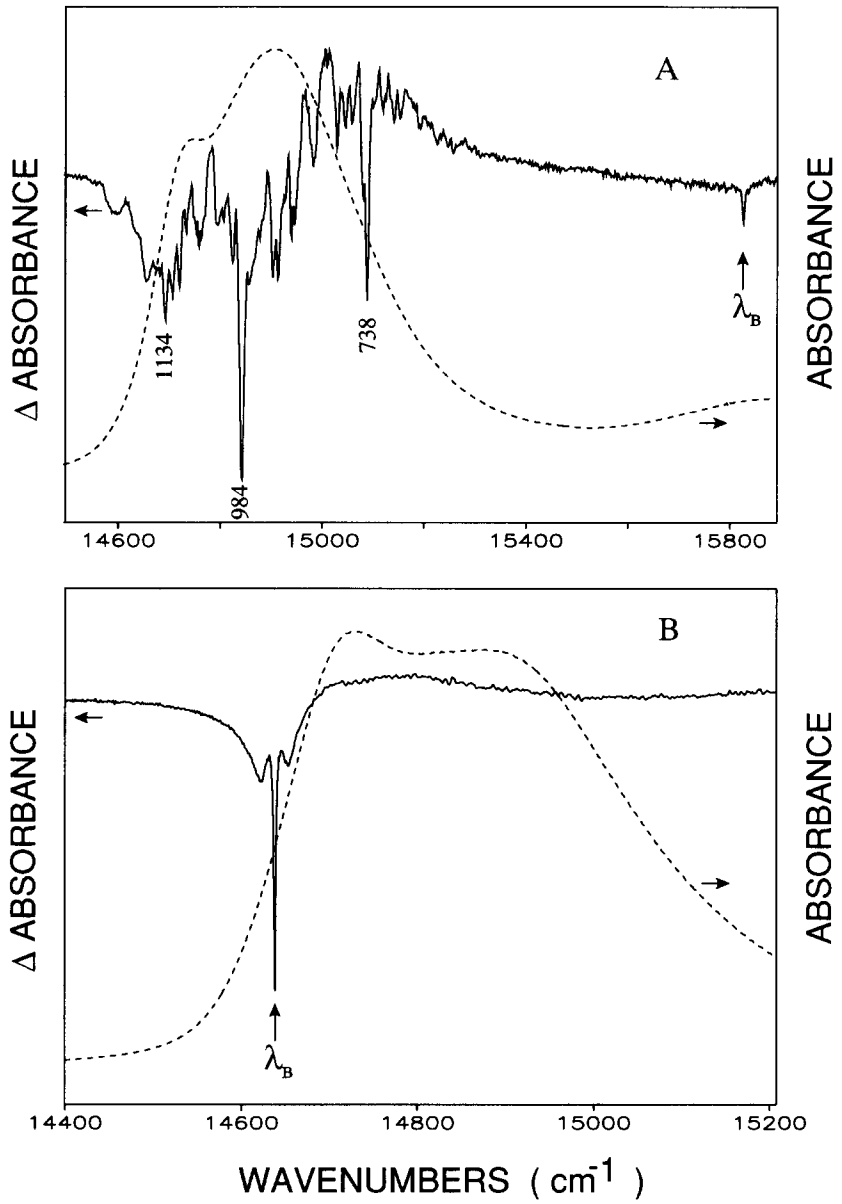

Fig. 3. (A) Vibronic satellite hole burned spectrum (solid line) of PS II reaction center. Several of the satellite holes (e.g., 738, 984 and 1134) are labeled with their excited state vibrational frequencies in cm^{-1}, $T_B = 4.2$ K, $\lambda_B = 632$ nm (unpublished data). Dashed line represents the 4.2 K absorption spectrum of PS II RC with ~0.05% Triton X-100 detergent. (B) Dashed spectrum corresponds to the absorption spectrum of PS II RC without Triton X-100. Solid line shows an example of non-photochemical hole burned spectrum of PS II RC burned in (0, 0) band at $\lambda_B = 682.5$ nm. The % ΔA change for the sharp zero-phonon hole is ~20%. Hole burning conditions: $I_B = 200$ mw/cm$_2$, $\tau_B = 20$ min; $T_B = 4.2$ K.

the isochromats relax to their respective zero-point positions in the (0, 0) band prior to hole burning. Two ZPH (at $(0,0)_A$ and $(0,0)_B$) are produced, which, in turn, lead to a hole at ω_L. The relative intensities of the former two and the latter depend, in part, on the Franck–Condon factors for vibrations α and β. A recent example (NPHB) is shown for the isolated PS II reaction center in Fig. 3A. Because the burn wavelength, λ_B, lies $\approx 1000\,cm^{-1}$ to higher energy of the

absorption origin region, the pseudo-vibronic hole structure is associated with vibrations possessing frequencies in the vicinity of $1000\,cm^{-1}$. The displacements of the vibronic 'satellite' holes from the burn frequency yield the excited state vibrational frequencies. The structure shown is due mainly to the accessory Chl *a* of the PS II reaction center (Tang et al. 1990c).

B. Theory of spectral hole profiles

The problem of understanding the interplay between the ZPH and PSBH and how the overall hole profile depends on the location of ω_B (laser burn frequency) within an absorption band whose width is contributed to by site inhomogeneity has been considered in considerable detail (Hayes et al. 1986, Won et al. 1987, Hayes et al. 1989, Lee et al. 1989). A summary of the theory developed in our laboratory is presented here.

To a good approximation the single site one-phonon absorption profile of impurity electronic transitions in amorphous hosts can often be viewed as a single broad profile which is displaced from the ZPL by ω_m ($\sim$20–30 cm^{-1}). With ν defined as the frequency of the ZPL, the single site absorption profile is of the form

$$L(\Omega - \nu) = e^{-S} l_0(\Omega - \nu) + \sum_{r=1}^{\infty} \frac{S^r e^{-s}}{r!} l_r(\Omega - \nu - r\omega_m) \quad (2)$$

in the low temperature limit. The l_r are line shape functions for zero- and multi-phonon absorptions. Ω is the frequency variable at which the function is evaluated. S is the Huang–Rhys factor which provides an estimate of the most intense member in the multi-phonon progression and $2S\omega_m$ is a reasonably accurate estimate of the Stokes shift. The Huang–Rhys factor characterizes the electron-phonon coupling. The coefficients of the line shape functions are the Franck–Condon factors. For coupling to the distribution of host phonons (lattice modes), the r-phonon profile is the result of convolving the one-phonon profile with itself r times. If the one-phonon profile is a Gaussian of width Γ, the r-phonon profile has a width $r^{1/2}\Gamma$; for a Lorentzian one-phonon profile, the r-phonon width is $r\Gamma$; in each case the r-phonon absorption is centered at $r\omega_m$. The one-phonon profile is the convolution of the phonon density of states and a frequency dependent electron-phonon coupling function and is generally not symmetric. A reasonable approach is to describe the asymmetric profile with a Gaussian and a Lorentzian for the low and high energy halves of the profile, respectively. This was done for all simulated spectra presented in this article.

Figure 4A presents a single site absorption spectrum calculated with Eq. (2) for $S = 1.8$, $\omega_m = 30\,cm^{-1}$, $\Gamma = 43\,cm^{-1}$ and $\gamma = 6\,cm^{-1}$, which is the homogeneous broadening of the ZPL due to an excited state lifetime of 0.9 ps. The centroid of the PSB is, as expected, displaced to higher energy of the ZPL by $\sim S\omega_m$. The ratio of the integrated intensity of the ZPL to that of the entire absorption spectrum is $\exp(-S)$, which is a consequence of the fact that the sum over all the Franck–Condon factors in Eq. (4). equals unity.

The absorption spectrum is the convolution of Eq. (2) with an appropriate zero-phonon site excitation distribution function (SDF):

$$A_0(\Omega) = \sum_{r=0}^{\infty} \frac{S^r e^{-S}}{r!} \int d\nu \, \frac{N_0(\nu - \nu_m)}{N} \times l_r(\Omega - \nu - r\omega_m) \quad (3)$$

where $N_0(\nu - \nu_m)/N$ is the probability of a site with a zero-phonon transition frequency equal to ν. A Gaussian centered at ν_m with a FWHM equal to Γ_I is the physically reasonable choice for N_0.

Figure 4B shows the absorption spectrum calculated with Eq. (3) for $\Gamma_I = 130\,cm^{-1}$ and the same values for the other parameters used for Fig. 4A. The fact that the calculated spectrum is not a symmetric Gaussian is due to the inclusion of the linear electron-phonon coupling.

Following a burn at ω_B with intensity I for a time τ, the number of sites remaining which absorb at frequency ν is given by $N_\tau(\nu - \nu_m) = N_0(\nu - \nu_m)\exp[-\sigma I \phi \tau L(\omega_B - \nu)]$, where σ is the absorption cross section and ϕ is the hole burning quantum yield. The burn laser frequency width is assumed to be narrow relative to the

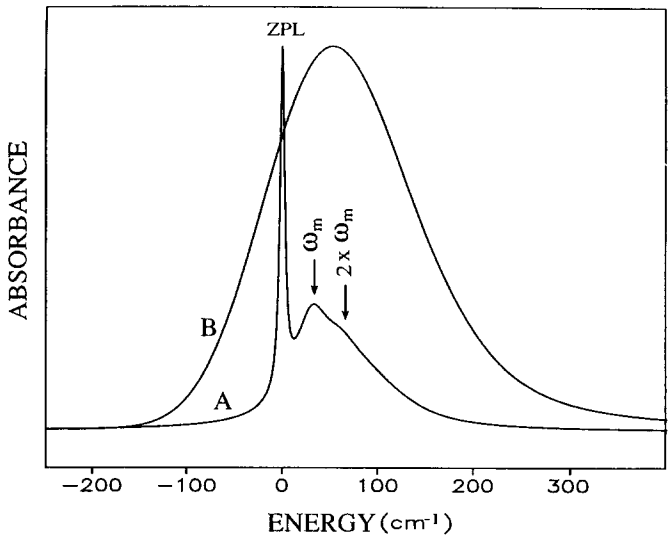

Fig. 4. (A) Single site absorption profile calculated according to Eq. (2) with $\omega_m = 30\,\mathrm{cm}^{-1}$, $\gamma = 6\,\mathrm{cm}^{-1}$, $S = 1.8$, $\Gamma = 3\,\mathrm{cm}^{-1}$. ZPL = Zero phonon line. (B) Absorption profile calculated according to Eq. (3) using parameters of A and $\Gamma_I = 130\,\mathrm{cm}^{-1}$.

homogeneous linewidth of the ZPL. The absorption spectrum after burning is thus

$$A_\tau(\Omega) = \sum_{r=0}^{\infty} \frac{S^r\, e^{-S}}{r!} \int d\nu\, N_0(\nu - \nu_m) \times e^{-\sigma I \phi \tau L(\omega_B - \nu)}\, l_r(\Omega - \nu - r\omega_m) \qquad (4)$$

Equation (4) does not allow for dispersive hole growth kinetics (i.e., $\phi = \phi(\tau)$ from a distribution of values for the hole burning rate constant) which is known to be important for NPHB (Jankowiak et al. 1987a, Kenney et al. 1990). However, in the short burn time limit ($\exp[-\sigma I\phi\tau L(\omega_B - \nu)] = 1 - \sigma I\phi\tau L(\omega_B - \nu)$) contributions due to dispersive kinetics may be neglected. Nor does Eq. (4) account for the anti-hole associated with NPHB (Lee et al. 1989), i.e., it is strictly applicable only to PHB and population bottle-neck hole burning. However, it is often the case that the anti-hole of NPHB can clearly be discerned in the experimental spectra (Gillie et al. 1989b, Lee et al. 1989) and its interference with the hole profile accounted for.

Model calculations performed with Eq. (4) are shown in Fig. 5 (for the parameter values used for Fig. 4) for $\omega_B = \nu_m$ (center of the SDF distribution), $\omega_B = \nu_m + 200\,\mathrm{cm}^{-1}$ and $\omega_B = \nu_m - 100\,\mathrm{cm}^{-1}$ (constant fluence). As ω_B is tuned from lower to higher energy, two characteristics are evident. Firstly, the spectrum becomes much less structured. In fact the highest energy burn closely resembles the absorption spectrum while the lowest energy spectrum resembles the single site absorption spectrum. This is because as the burn frequency increases the probability of exciting multiphonon transitions increases. Secondly, the centroid of the hole shifts with burn frequency. This shift is approximately $150\,\mathrm{cm}^{-1}$ and is directly related to the ratio of Γ_H to Γ_I (Hayes et al. 1988). As this ratio increases, it is observed that the shifting becomes less pronounced.

The extension of the theory to include more than one type of low frequency intermolecular mode is quite straightforward (Johnson et al. 1991b). We present here only simulated spectra for the case where both the protein phonons and a localized intermolecular mode couple linearly to the electronic transition. The frequency and Huang–Rhys factor of the latter are designated as ω_{sp} and S_{sp} so that the total optical reorganization energy is $\sim S\omega_m + S_{sp}\omega_{sp}$. For the calculations we consider a system for which $S_{sp} = 1.5$, $\omega_{sp} = 125\,\mathrm{cm}^{-1}$, with the values of Γ_I and the linear electron-phonon coupling parameters as given earlier. The single site absorption spectrum is shown in Fig. 6A (see Table 1 for details concerning the lifetimes employed for the 1- and

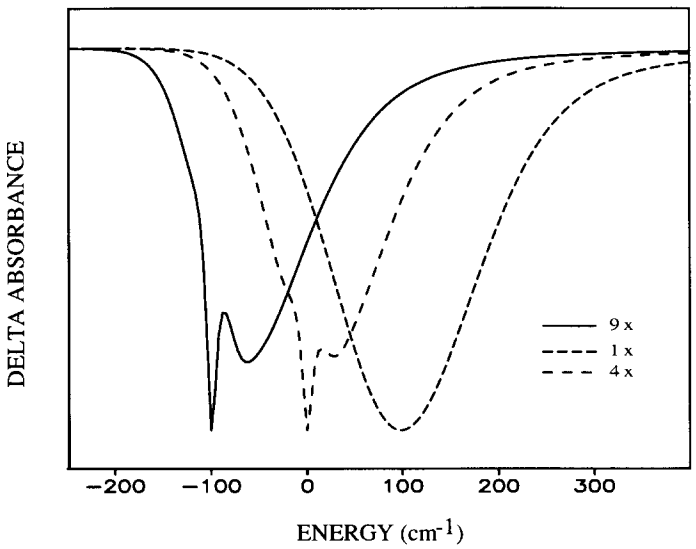

Fig. 5. Three constant fluence hole burned spectra calculated from Eqs. (4)–(3) with parameters of Fig. 4. Holes burned at (from left to right) $-100\,cm^{-1}$, $0\,cm^{-1}$, $200\,cm^{-1}$ relative to the site distribution function maximum, v_m. Inset refers to relative depths of the holes (i.e., the $-100\,cm^{-1}$ burn is nine times less intense than the $0\,cm^{-1}$ burn).

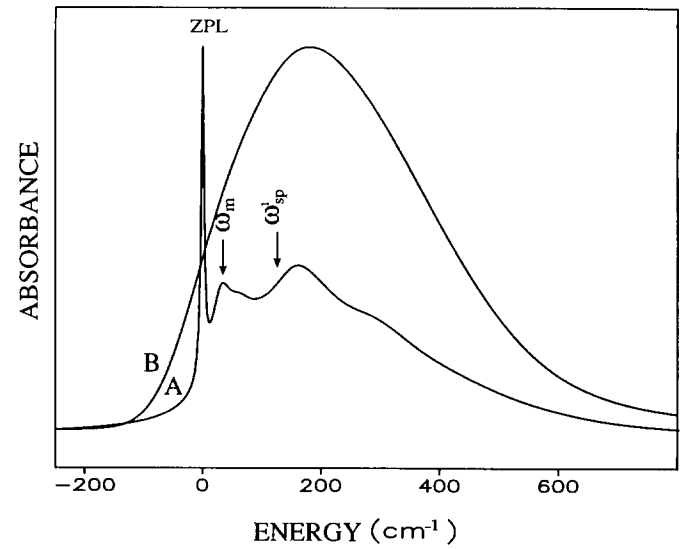

Fig. 6. (A) Single site absorption profile including coupling to the marker mode. Parameters as in Fig. 4A with $S_{sp} = 1.5$ and $\omega_{sp} = 125\,cm^{-1}$. ω^1_{sp} locates the position of the first overtone of the marker mode displaced $125\,cm^{-1}$ from ZPL. (B) Absorption profile calculated as in Fig. 4B.

higher quantum levels of the ω_{sp}-mode). The calculated absorption spectrum is given in Fig. 6B. Figure 7 shows three hole burned spectra for $\omega_B = \nu_m$, $\nu_m + 200$ and $\nu_m - 100$. Comparison of these holes to those in Fig. 5 reveals that the shifting of the centroid of the holes in Fig. 7 ($\sim 70\,cm^{-1}$) has decreased. This is because the homogeneous broadening has increased, changing the Γ_H to Γ_I ratio (about 4.5 times greater than in the single mode case).

Table 1.

	ω_{sp}[a]	ω_m	S_{sp}	S	Γ[b]	Γ_t[c]	$\Sigma S_i \omega_i$
P960[d]	135[i]	25	1.1	2.1	40	120	200
P870 (R-26)[d]	115[i]	30	1.5	2.2	30	170	240
P870 (deut.)[e]	125[i]	30	1.5	1.8	43	130	242
P700[f]	35–50		6–4		60	100	200
P680[g]	–[h]	26	–	1.9	25	120	50

[a] All frequencies and widths are cm^{-1}. [b] Total width of 1-phonon profile which is taken as a Gaussian and Lorentzian for the low and high energy halves. For P870 (deut.) the Gaussian and Lorentzian half-widths are 15 and 25 cm^{-1}, respectively. [c] The narrowest P960, P870 (R-26) and P870 (deut., wild-type) bands measured in our laboratory carry FWHM of 420, 470 and 380 cm^{-1}. [d] From Johnson et al. (1990). [e] Deut. = fully deuterated. From Lyle et al. (1991). [f] From Gillie et al. (1989). The P700 hole profile is devoid of any structure and, thus, a single mean phonon frequency was used for simulations, see text. [g] From Jankowiak et al. (1989). [h] The special pair marker mode (ω_{sp}) is totally absent in the P680 hole spectrum. [i] Allowance for 100 fs relaxation of ω'_{sp} is made in the simulations; the $\omega^j_{sp}(j>1)$ levels are allowed to decay in 100/j fs (Fermi-Golden rule prediction with cubic anharmonicity).

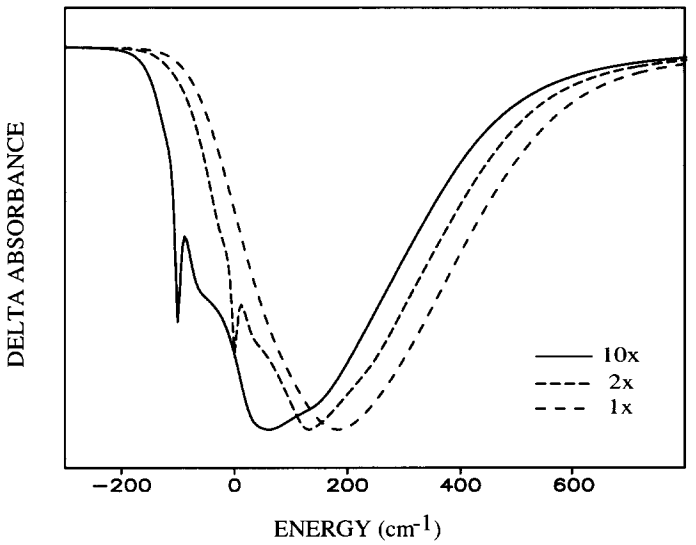

Fig. 7. Three constant fluence hole burned spectra calculated with the parameters of Fig. 5.

C. Experimental

Absorption and hole burned spectra presented in this article were obtained using a Bruker IFS 120 HR Fourier-transform infrared (visible) spectrometer which has a resolution power of 10^6. Optical densities of the samples were adjusted to <0.8 (at the maximum of the absorption band of interest) by dilution in a buffered glycerol/H_2O glass-forming solvent. These samples were quickly cooled to 4.2 K in a Janis Model 8-DT Super Vari-Temp liquid helium cryostat. Any of the several laser systems (Coherent CR699-21 ring dye laser or Coherent CR899 cw Ti:Sapphire laser or a pulsed Ti:Sapphire (Excel Technology) or a Lambda Physik FL2000 excimer dye laser) available in the laboratory provided the burn radiation.

III. Applications

A. Reaction center complexes of purple bacteria

(i) Absorption and hole spectra

The structures of the reaction center (RC) of *Rps. viridis* (Deisenhofer et al. 1984, 1985, Michel et al. 1986a, 1986b) and *Rb. sphaeroides*

(Allen et al. 1986, Chang et al. 1986, Yeates et al. 1988) have led to even greater activity directed towards understanding the primary charge separation process that is triggered by excitation of the primary electron donor states P960* and P870*, respectively. The structural arrangement of the cofactors for *Rb. sphaeroides* R-26 is given in Fig. 8 while the 4.2 K absorption spectrum of the Q_y-region of the perdeutero-RC of *Rb. sphaeroides* (wild type) is shown in Fig. 9. P870 is peaked at 896 nm, with the bands from the two BChl *a* and two BPheo *a* monomers located at 802 and 756 nm, respectively. It is generally accepted that the lowest energy dimer component of the special pair (P) contributes very significantly to P870. Low temperature linear dichroism studies (Vermeglio et al. 1982) have led to an assignment for the low energy shoulder of the BChl *a* monomer band as the upper dimer component (P_+). The same assignment was made for the better resolved low energy shoulder of the BChl *b* monomer band of *Rps. viridis*. Our

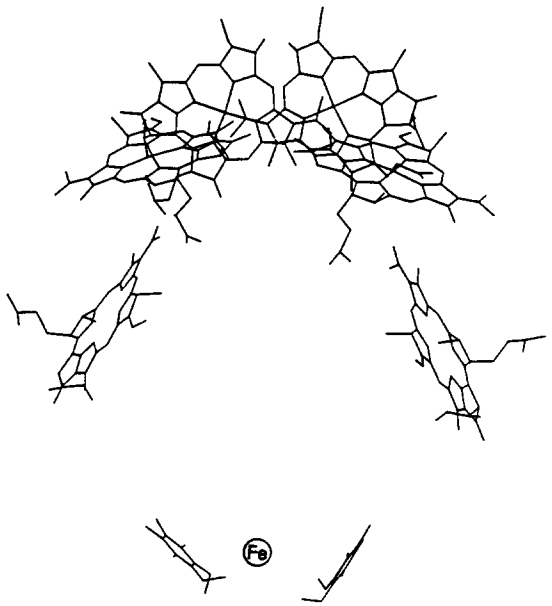

Fig. 8. Structural arrangement of the cofactors of *Rb. sphaeroides*. The special pair of BChl *a* monomers overlapping at ring I is shown at the top.

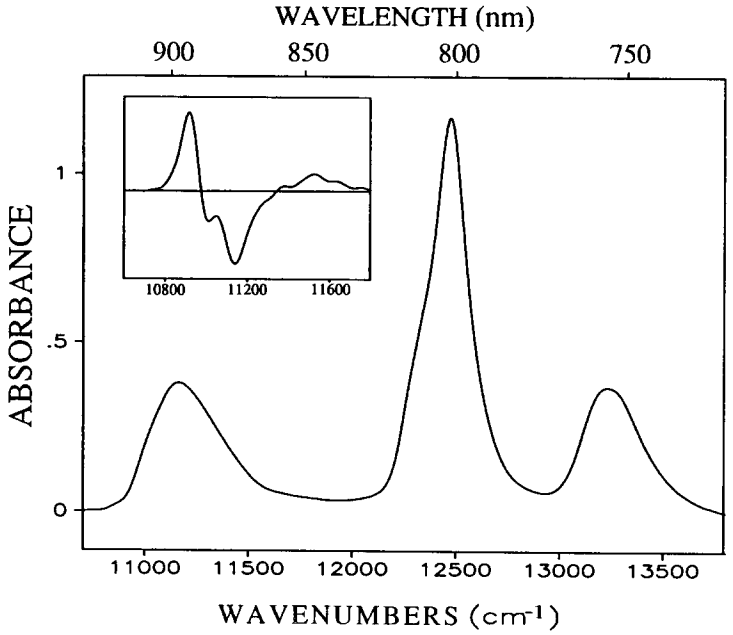

Fig. 9. Experimental absorption spectra of the Q_y region of the deuterated wild type *Rb. sphaeroides* at $T = 4.2$ K. Inset: Second derivative of the P870 spectral region.

polarized photochemical hole burned spectra for both RC, obtained with the probe polarization at 0, 30, 60 and 90° relative to the polarization of the burn laser, confirmed that the low energy shoulder carries a polarization which is close to perpendicular to that of the primary donor state (P) (unpublished results of S. Johnson and D. Tang). Additional support for the above assignment can be found in the dependence of the Q_y-hole spectra on λ_B, burn wavelength, as it is tuned through P870 (P960) (Tang et al. 1990b). As will be illustrated below, the center of gravity of the broad P870 hole shifts to the blue as the burn frequency is increased from the low energy side of P870 (an effect first observed by Boxer and coworkers (Boxer et al. 1986a)). Tang et al. (1990b) showed that the satellite hole associated with the aforementioned low energy shoulder *tracks* the P870 hole, meaning that the site distribution functions of the low energy shoulder state and P870 are positively correlated. This type of correlation is expected for dimer states.

Figure 9 shows that the primary donor state absorption band is significantly broader than those of the 'monomer' cofactors. This is even more apparent for *Rps. viridis* for which the two BPheo *b* bands are resolved (Tang et al. 1990b). Identification of the origin of the additional width was recognized as important in the first photochemical hole burning studies of P870 (Meech et al. 1985, Boxer 1986a) and P960 (Boxer 1986b) based on the production of metastable P^+Q^-. In these works, broad and structureless holes were observed with widths approaching those of the absorption bands. Two theoretical models appeared shortly thereafter, one which attributed the structureless broad hole to an ultra-fast *electronic* relaxation (<100 fs) of P* prior to formation of P^+BPheo^- (Won et al. 1988a, 1988b) and the other which attributed the large homogeneous broadening of P870 (P960) to strong linear electron-phonon coupling (Hayes et al. 1986, 1988). An important distinction between the two models is that the former predicted that a narrow ZPH coincident with ω_B should not be observed while the latter predicted that it could be. Subsequent studies of high quality samples revealed the existence of a weak ZPH and, in addition, structure associated with a Franck–Condon progression of a special pair *intermolecular* ('marker') mode (ω_{sp}) (Johnson et al. 1989c, Tang et al. 1989). For P870 and P960 of *Rb. sphaeroides* and *Rps. viridis*, the ω_{sp}-values were found to be 115 and 135 cm^{-1}, respectively.

In Fig. 9 the origin band (ω_{sp}^0) of the marker mode corresponds to the low energy shoulder of P870 with the 1-quantum transition, ω_{sp}^1, located near the maximum of P870 (see insert spectrum). Figure 10 shows two of our recently obtained hole spectra (Lyle et al. 1991) for $\lambda_B = 883$ and 910 nm. As was the case in our earlier studies, the ZPH coincident with λ_B could only be observed for λ_B located in the near vicinity of P870's low energy shoulder (i.e., under optimum line narrowing conditions). The fits given in Fig. 10 were obtained with the parameter values given in Table 1 and $\gamma = 6\ cm^{-1}$, which also contains the parameter values reported earlier (Johnson et al. 1990) for P960 and P870 of the R-26 mutant. Thus, P* (P_-) couples to two types of phonons: the marker mode, which is a localized phonon (ω_{sp}, S_{sp}) involving intermolecular motion of the monomers of the special pair; and low frequency protein phonons (ω_m, S). It was the T-dependence of the ZPH intensity for P870 of the R-26 mutant which led to a value of $\omega_m = 23 \pm 4\ cm^{-1}$ (Johnson et al. 1990). With regard to the theoretical simulations, it should be emphasized that the λ_B-dependence of the hole spectra together with P's absorption band must be accounted for with one and the same set of parameter values and that the ratio of the site inhomogeneous broadening, Γ_I, to the homogeneous broadening $\Gamma_H \sim S\omega_m + S_{sp}\omega_{sp}$ is *critically* important for understanding how the center of gravity of the overall hole profile of P shifts as λ_B is varied. Furthermore, the simulations should be viewed as providing a refinement of the values for S, ω_m, S_{sp}, ω_{sp} and Γ_I which can be quite accurately estimated from the experimental data. Of course, Γ_I is somewhat sample (host) dependent. From Table 1 we see that the total optical reorganization energy is about 200 cm^{-1}, which is over an order of magnitude greater than the values determined for antenna Chls and BChls even when they are strongly exciton coupled (Johnson et al. 1991). Thus, the linear electron-phonon coupling for P* is strong ($S_{total} = S + S_{sp} \sim 3$), while for antenna pigments it is weak ($S_{total} < 1$). Moreover, a high frequency phonon like the special pair marker mode is not observed

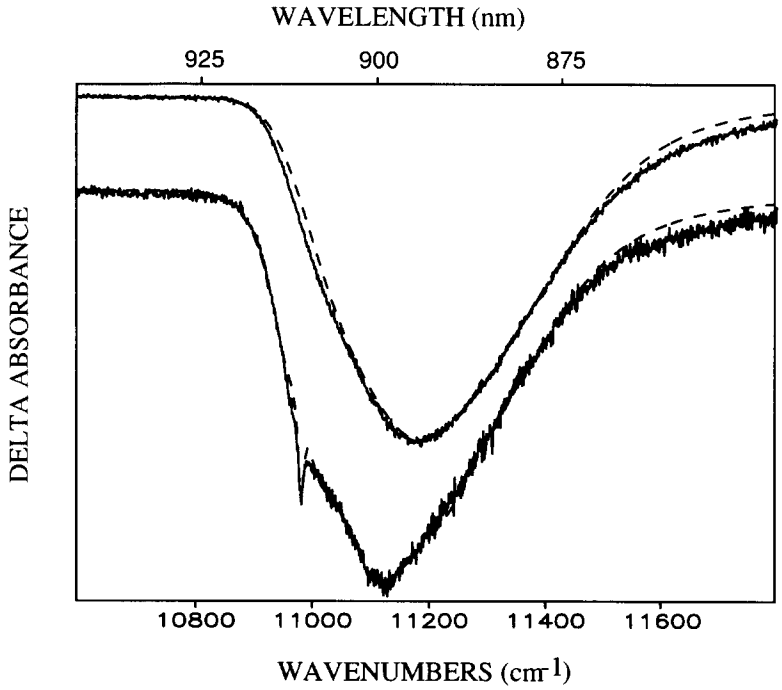

Fig. 10. Experimental (solid lines) and calculated (dashed lines) for two different burn wavelengths in P870. Lower set of curves $\lambda_B = 910$ nm and the upper set $\lambda_B = 883$ nm.

for antenna pigments. Since studies of the neutral excitonic $\pi\pi^*$ dimer states of organic crystals such as anthracene (Port et al. 1979) and naphthalene (Robinette et al. 1978) had shown that the exciton-phonon coupling is *weak* but that the coupling of charge-transfer (CT) states of 1:1 π-molecular donor-acceptor complexes is very strong (Haarer 1974), it was suggested that P* must possess a significant amount of CT character (Johnson et al. 1990). This is consistent with Stark data (Losche et al. 1987, Lockhart et al. 1988, 1990) as well as electronic structure calculations (Warshel et al. 1987).

(*ii*) *The low temperature absorption spectrum of P870 for a* single *RC*

The parameter values given in Table 1 can be used to calculate the low temperature absorption spectrum of the special pair P state for a *single* RC. This spectrum for P870 of the perdeutero-RC is shown in Fig. 6 (a) with the marker mode progression clearly evident. Building on the 'origin' ZPL (at $\omega = 0\,\mathrm{cm}^{-1}$) is the phonon sideband (PSB) with $\omega_m = 30\,\mathrm{cm}^{-1}$ and $S = 1.8$. The ω_{sp}^1 and higher marker mode progression numbers should be measured relative to the PSB of the above origin ZPL. The reason is that the calculation allows for ultra-fast vibrational relaxation of the marker mode, 100 fs corresponding to an uncertainty broadening of $50\,\mathrm{cm}^{-1}$ (relative to a homogeneous lifetime broadening of the origin ZPL of $6\,\mathrm{cm}^{-1}$), cf. subsequent subsection for a discussion of the ultra-fast relaxation. Thus, the ZPLs for the 1- and higher marker mode progression members are broadened to an extent which makes them unobservable, although they contribute intensity to the low energy side of the 1- and higher quantum marker mode profiles.

The single RC spectrum of Fig. 6 was used with Eq. (3) and $\Gamma_I = 130\,\mathrm{cm}^{-1}$ to compute the absorption spectrum of Fig. 6. The latter provides an acceptable fit to the experimental absorption profile of P870 (Lyle et al. 1991).

(*iii*) *Electronic relaxation time of P* from a single phonon-vibration level: Implication for thermalization kinetics*

Theory (Hayes et al. 1988) predicts that the intensity of the ZPH of the type shown in Figs. 7 and 10 relative to the intensity of the entire hole associated with the ω_{sp}^0 transition is $\sim\exp(-2S)$. For $S = 1.8$ (see Table 1), $\exp(-2S) = 0.027$,

which can be thought of as the Franck–Condon factor for the ZPH. The corresponding FC factor for the ZPL line is $\exp(-S) = 0.165$. The smallness of this number is important for future femtosecond photon echo experiments on P since the levels excited in such experiments would be predominantly multi-phonon in nature. However, despite the unfavorable FC factor for the ZPL, it is precisely the *total* zero-point level of P which the observed ZPH corresponds to. The ZPH width for P870 of the perdeutero-RC is $6\,cm^{-1}$ which corresponds to a lifetime for P870* of 0.9 ps at 4.2 K. Within our experimental uncertainties, this is the same as the lifetime for the perproto-RC of the R-26 mutant (Johnson et al. 1989c). Thus, we have confirmed, by measurements on the total zero-point level of P*, that deuteration has little effect on the primary charge separation kinetics (Breton 1988a).

There is good agreement between the time domain (10 K) and hole burning (4.2 K) values for the lifetime of P* for all RC we have studied (Johnson et al. 1989c, Tang et al. 1989). The agreement is interesting since the excitation wavelengths utilized in the time domain measurements on P870 prepare phononically and marker mode 'hot' P870*. According to non-adiabatic electron transfer theory (Jortner 1980, Bixon et al 1982), one would not expect the above agreement *unless* thermalization of all relevant phonon modes occurred on a time scale that is fast relative to primary charge separation. There are other hole burning results which speak to this issue. Conspicuously absent in all of our hole spectra for P of *Rps. viridis* and *Rb. sphaeroides*, which exhibit the ZPH coincident with λ_B located in the low energy shoulder of the P absorption band, are the 'companion' higher energy satellite ZPHs of the marker mode progression. Indeed, our simulations (not shown), in which the lifetimes of the ω^1_{sp}, ω^2_{sp}, etc. levels are set equal to the low temperature lifetime of P* show pronounced ZPH progressions with the ZPH of the ω^1_{sp} transition being the most intense. To eliminate the marker mode progression ZPHs, it is necessary to invoke ultra-fast vibrational relaxation in ~100 fs (there are *no* data which indicate that P* undergoes *electronic* relaxation faster than the formation of $P^+B_L^-$; in fact, the hole burning data prove that such relaxation does not occur from total zero-point (Tang et al. 1990b)).

(iv) The phonons and their role in charge separation

On the basis of the hole burned spectra of several systems it is apparent that the coupling of low frequency phonons ($\omega_m \sim 20$–$30\,cm^{-1}$) to the Q_y-transitions of cofactors of antenna and RC complexes is ubiquitous. Importantly, modes of this frequency couple most effectively to the $S_1(\pi\pi^*)$ states of a variety of chromophores in organic glasses and polymers. Thus, they are likely to be more or less spatially extended phonons of the 'soft' organic host rather than a localized phonon (libration) of the chromophore. For this case the one-phonon profile of the ZPL is governed by $D(\omega)g(\omega)$, where $g(\omega)$ is the phonon density of states of the host and D is a frequency dependent coupling function. For protein complexes the width of this product is about $30\,cm^{-1}$. The picture which has emerged for the coupling strength is that it is weak for Chls and BChls of antenna but moderately strong ($S \sim 2$) for P* of the RC of purple bacteria and PS II of green plants.

The coupling strength for pure charge-transfer transitions such as P* BChl BPheo$\rightarrow P^+BChl^-$ BPheo and P^+BChl BPheo$^-$ of purple bacterial RC must be considerably stronger than for the P*$\leftarrow$P optical transition since both electron-transfer processes are accompanied by a large dipole moment change (Ogrodnik 1991). Therefore, protein phonons of the type above should contribute to the Marcus reorganization energy and be a factor in the temperature dependence of the primary charge separation kinetics which *accelerates* with decreasing temperature (Kirmaier et al. 1985, Fleming et al. 1988). Recently, an Einstein model with a single phonon was employed to interpret the T-dependence of primary charge separation for *Rb. sphaeroides* and *Rps. viridis* (Bixon et al. 1989). For both, the theoretical fit with $\omega = 80\,cm^{-1}$ is quite satisfactory for $T \lesssim 200$ K. The model assumed that P^+BChl^- serves as a virtual state (lying higher in energy than P*) in a super exchange mechanism for production of P^+BPheo$^-$. For an adiabatic energy gap between the latter charge-separated state and P* of $\sim -2000\,cm^{-1}$, the Huang–Rhys

(S) factor required by energy conservation is ~ 25 (very strong coupling). It is interesting that our theoretical simulations of the first reported and unstructured hole spectra of P870 and P960 (Boxer et al. 1986a, 1986b) utilized a mean phonon frequency of $80\,cm^{-1}$ (Hayes et al. 1988). We understand now that this frequency is the mean of the frequencies of the special pair marker mode and the protein phonons. Fits to the temperature dependence of primary charge separation for P870* and P960* obtained with a two mode model (ω_{sp} and ω_m) would be as satisfactory as those reported by Bixon and Jortner. However, the question of whether the marker mode plays an important role in the temperature dependence is problematic. There are several reasons for this including that Bixon and Jortner did not consider the contribution from intramolecular modes to the Marcus reorganization energy and that the question of the role of P^+BChl^- (virtual or real intermediate state) has very recently again become controversial (Holzapfel et al. 1990). It has been suggested that (Ogrodnik et al. 1991) P^+BChl^- may serve as both a virtual and a real (intermediate) state in the formation of P^+BPheo^- with the relative contributions being T-dependent, which further 'muddies' the interpretation of the T-dependence of the initial phase of charge separation. Nonetheless, it is clear that low frequency phonons do play an important role in mediating charge separation.

We turn next to the question of the dynamical nature of the special pair marker mode. Both the frequencies and large S-values ($S_{sp} \geqslant 1$) are entirely inconsistent with this mode being a Franck–Condon active intramolecular vibration of BChl (Tang et al. 1990b). It follows, therefore, that the marker mode is intermolecular in nature (a 'localized' phonon) intimately associated with the special pair of bacterial RC. Furthermore, the value of ω_{sp} is greater for P960* than P870* while the distance between the overlapping pyrrole rings I of the special pair of *Rps. viridis* (Deisenhofer et al. 1984) and *Rb. sphaeroides* (Allen et al 1987) is ~3.0 and 3.5 Å, respectively . These results suggest that coupled librational motion of the two monomers of the pair are likely to be a significant contributor to the dynamics. Neighboring residues and, perhaps, the monomers $BChl_L$ and $BChl_M$ could also contribute to the marker mode coordinate. When this coordinate is identified by electronic structure calculations, it should be possible to calculate the geometry of the special pair and its immediate surroundings for the Q_y-state from the experimental S_{sp}-value.

Although the marker mode must contribute to the Marcus reorganization energies for charge separation from P* (it is only a question of the relative magnitude of its contribution), it does not appear that the marker mode serves as a *promoting* vibration for electron-transfer, i.e., as a phononic 'switch.' since, were this the case, primary charge separation would accelerate with increasing temperature.

Following the hole burning studies it proved possible to obtain a resonance Raman spectrum of the RC of *Rb. sphaeroides* with the excitation laser frequency located in the near vicinity of the low energy shoulder of P870 (the ω^1_{sp} band). Two rather broad ($\sim 30\,cm^{-1}$) bands at 102 and $138\,cm^{-1}$ were observed and assigned to the special pair (Donohue et al. 1990). Thus, it is possible that the $115\,cm^{-1}$ marker band identified from the hole spectra is contributed to by two bands rendered unresolvable, in part, by the broadening from the linear electron-phonon coupling. In fact, the hole spectra for P960 of *Rps. viridis* show some evidence for the ω^1_{sp} hole being due to more than one vibration (see Fig. 5 of Tang et al. 1990b). The two intermolecular modes might correspond to symmetric and antisymmetric vibrations of a single librational (hindered rotation of coupled molecules) degree of freedom. Interestingly, the above two Raman bands could not be observed when the laser was tuned to higher energy in the P870 absorption profile. This is consistent with the results of the hole burning experiments which indicate that the marker mode (ω_{sp}) and its overtones relax in about 100 fs.

(*v*) *Deuterated reaction centers of* Rb. sphaeroides

Comparison of the hole spectrum of Fig. 10 and others for the perdeutero-RC of wild type *Rb. sphaeroides* with the published spectra for the perproto-RC (R-26 mutant) (Johnson et al. 1990) reveals that the ZPH and associated struc-

ture of the former are the better resolved. This is due primarily to the fact that Γ_I for P870 of the perdeutero-RC is smaller than for the perproto-RC (see Table 1) which, in turn, leads to a FWHM for P870 of the former of only 380 cm^{-1} at 4.2 K. From Table 1 it can be seen that the values of S, ω_m, S_{sp} and ω_{sp} for P870 of the perproto-RC differ from those reported earlier for the perproto-RC. The differences are not viewed as significant at this time since they lie within the ranges of uncertainties for these parameters (Johnson et al. 1990). Therefore, we may conclude that deuteration has at most a small effect on the underlying structure of P870, i.e., on all physical parameters except Γ_I. It is hardly surprising that low frequency phonons and their electron-phonon coupling should not be strongly effected by deuteration. With our interpretation for the dynamics of the marker mode, one would not expect its frequency to be subject to a significant deuteration shift.

B. Reaction centers of green plants

Hole burning has been applied to the primary electron donor states P700* and P680* of the RC of PS I (Gillie et al. 1989a) and PS II (Tang et al. 1990a), respectively. For the former, enriched (35–45:1; Chl *a*:P700) PS I particles containing the full set of electron acceptors A_0, A_1, F_x and F_A/F_B were utilized. At liquid helium temperatures, $P700^+$ F_A/F_B^- is formed irreversibly so that persistent photochemical holeburning could be performed on P700, which is clearly discernible as a weak low energy shoulder of the main 670 nm absorption band at 1.6 K. D1–D2–cyt b_{559} RC complexes of PS II isolated by two distinct procedures were studied. For both, the quinone electron acceptors are absent so that population bottleneck hole burning via ^{3}P680* was employed for the study of P680.

(*i*) *The D1–D2–cyt* b_{559} *reaction center complex of PS II*

The PS II RC of plants and the RC of purple bacteria appear to share structural and functional similarities (Michel et al. 1986a). For example, nucleotide and amino acid sequence homology exists between the D1 and D2 subunits of the PS II RC and the L and M subunits of the bacterial RC. The original preparation of the isolated D1–D2–cyt b_{559} RC was reported to contain 4–5 Chl and 2 Pheo (Nanba et al. 1987). The correct composition is now subject to debate and, for example, Chl/Pheo ratios of 6:2 (Kobayashi et al. 1990) and 10–12:2–3 (Dekker 1989) have been reported. However, it was recently shown that (Tang et al. 1990c) the low temperature absorption and hole burned spectra of two distinctly different preparations, McTavish et al. (1989) and Dekker et al. (1989), are very similar.

The isolated RC of PS II provides a rich system for spectral hole burning because the accessory Chl *a* and Pheo *a* (active in electron transfer) undergo facile persistent non-photochemical hole burning while P680 can be studied by transient population bottleneck hole burning. We shall focus on P680 and simply state some of the other more interesting findings: the lifetimes of the accessory Chl *a* and Pheo *a* (active) states due to downward energy transfer are 12 and 50 ps, respectively; the electron-phonon coupling for both these states is weak; the P680 and active Pheo *a* absorption bands (determined from non-line narrowed hole spectra) are degenerate at 681.5 nm but the zero-point level of the Q_y-state of Pheo *a* lies ~25 cm^{-1} higher in energy than that of P680 at 4.2 K; and Γ_I for P680 and the Q_y-band of Pheo *a* is ~100 and ~105 cm^{-1}, respectively.

The low temperature absorption spectra of the D1–D2–cyt b_{559} RC and D1–D2–cyt b_{559}-CP47 complexes are shown in Fig. 11. In Fig. 11B the most prominent feature at ~679 nm is due to P680 (and to a lesser extent the active Pheo *a*) while the broader band at ~673 nm is due mainly to the accessory Chl *a* of the RC. Since the proximal antenna complex CP47 binds 20–25 Chl *a*, it dominates the absorption band at ~675 nm in Fig. 11A. The isolated CP47 complex has absorptions at ~663, 670, 676 and 683 nm (Ghanotakis et al. 1989)

Rather than reproduce here our recently published hole spectra for P680 of the isolated D1–D2–cyt b_{559} complex (Tang et al. 1990a), we show one of our unpublished transient hole spectra in Fig. 12 of the RC bound to CP 47. This spectrum was obtained following saturation of

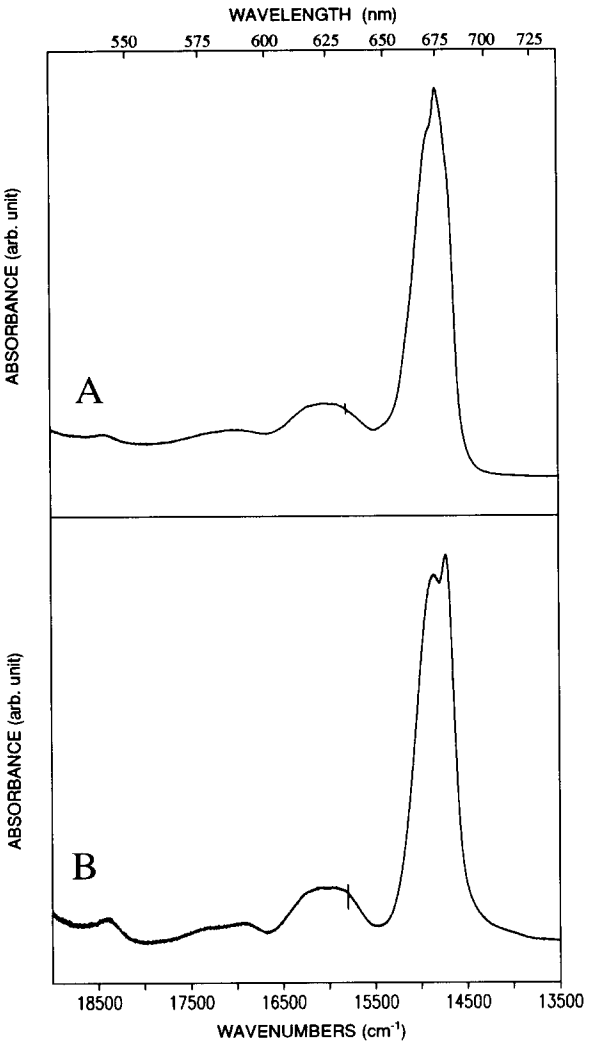

Fig. 11. Absorption spectra ($T = 4.2$ K) of (A) D_1/D_2/cyt b_{559}/CP47 reaction center complex and (B) D_1/D_2/cyt b_{559} reaction center complex.

the persistent NPHB due to pigments other than P680 and, except for the relatively weak and broad feature at ~678 nm, it (and transient spectra obtained with λ_Bs in the near vicinity of 683 nm) bear a striking resemblance to the line-narrowed hole spectra for P680 of the preparations devoid of CP47. The ZPH at 683.0 nm carries a width of 6 cm^{-1}, which is the same as that reported earlier (within experimental uncertainty of ±10%). The broader features at $\lambda_B \pm \sim 20\ cm^{-1}$ are the phonon sideband holes of the ZPH; their shapes and intensities are similar to those for the D1–D2–cyt b_{559} complex. We

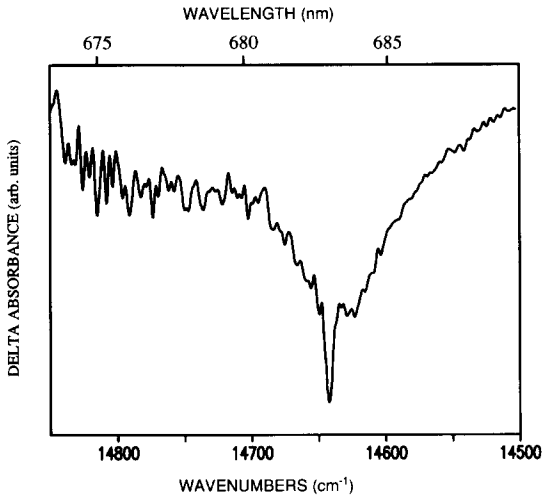

Fig. 12. Transient hole burned spectrum of P680 at 4.2 K for the D_1/D_2/cyt b_{559}/CP47 reaction center complex with λ_B = 683 nm.

conclude, therefore, that the transient hole in Fig. 12 is due to P680. (The relatively broad feature at ~678 nm is presumably due to a transient contribution of CP47. Experiments on the isolated CP47 complex are planned to check this). Our preliminary theoretical simulations for P680 yield $S \sim 2$, $\omega_m \sim 20\ cm^{-1}$ and $\Gamma_1 \sim 100\ cm^{-1}$. As emphasized in our earlier work (Tang et al. 1990a), the hole spectra of P680 are *devoid of the marker mode progression* observed for the primary donor band of the bacterial RC.

The P680 ZPH width corresponds to a P680* lifetime of 1.9 ± 0.2 ps (Jankowiak et al. 1989). Time domain measurements yielded lifetimes of 2.6 ± 0.6 and 1.4 ± 0.2 ps at ice temperature and 15 K, respectively (Wasielewski 1989a, 1989b). These kinetics and their temperature dependence are similar to those for P870*. The significance of the agreement between the hole burning and time domain values for the lifetime of P* has already been discussed.

Spectral hole burning has revealed two major differences between the RC of PS II and the RC of purple bacteria: whereas the Q_y-states of the accessory BChl and BPheo of the bacterial RC undergo downward energy transfer in ~30 fs (Jankowiak et al. 1989), the Q_y-state of the accessory Chl and Pheo (active) of the PS II RC decay in 20 and 50 ps, respectively (Tang et al., 1990c). It was also shown that the detergent

Triton X-100 (but not dodecyl maltoside) severely disrupts downward energy transfer from the accessory Chl. Furthermore, the marker mode progression observed for P870 and P960 is absent for P680 (however, the coupling to the low frequency phonons is the same). Thus, the existence of the special pair marker mode is *not* a necessary condition for charge separation to occur in ~2 ps. Furthermore, ultra-fast energy transfer of the Q_y-states of the accessory cofactors does not necessarily go hand in hand with picosecond charge separation kinetics.

The absence of the marker mode for P680 raises the question of whether or not P680 is a special pair or dimer. Based on the hole spectra, the energy gap between P680* and the Q_y-state of the accessory Chl *a* of the RC is $\sim 220\,cm^{-1}$ at 4.2 K, which is considerably smaller than the corresponding values of ~1600 and $\sim 2000\,cm^{-1}$ for *Rb. sphaeroides* and *Rps. viridis* (the dimer state splittings for these purple bacteria are slightly smaller). If P680 is a special pair, then the above observations indicate that the monomers of the pair are weakly exciton coupled relative to P870 and P960, but that the geometry (relative orientations of the Q_y-transition dipoles) is such as to render one of the dimer states dipole forbidden (very weakly absorbing). This does not exclude from consideration the basic geometry found for the special pair of bacterial RC; for example, the two monomers could 'slip' further apart to increase the Mg..Mg distance from ~7 Å and reduce the overlap of rings I of the two BChl molecules. A slip translation of $\geqslant 3$ Å would eliminate skeletal overlap of rings I. This tentative structural model might explain the total disappearance of the marker mode for P680 provided the marker mode involves libration-induced displacements of the overlapping rings I.

From Table 1 we observe that the values of S and ω_m for P680 are essentially identical to those for P870 and P960 of *Rb. sphaeroides* and *Rps. viridis*. As emphasized earlier, $S\omega_m \sim 50\,cm^{-1}$ for the primary electron donor states is significantly larger than the measured values for antenna Chls and BChls ($S\omega_m \sim 10$–$15\,cm^{-1}$). This was explained in terms of the relatively large dipole moment change for primary donor states, *vide supra*. However, since the marker mode (ω_{sp}) is not active for P680, P680*'s optical reorganization energy is ~60–70% smaller than those of the primary donor state of bacterial (also PS I, *vide infra*) RC. This suggests that the dipole moment change for P680* is significantly smaller than for P* of the bacterial RC, which is supported by preliminary Stark data (Lösche et al. 1988).

(ii) The primary electron donor state, P700, of PS I*

Our work (Gillie et al. 1989a) on the photochemical hole burning spectroscopy of the primary donor state absorption band, P700, of PS I has recently been reviewed (Johnson et al. 1991b). Thus, our discussion will cover only a few salient results. Independent of λ_B within the P700 band, the hole profile is broad and structureless with a FWHM of $\sim 300\,cm^{-1}$ and is devoid of a ZPH. The dependence of the center of gravity of the hole on λ_B led to values for Γ_I and the total optical reorganization energy of $\sim 100\,cm^{-1}$ and $\sim 200\,cm^{-1}$, respectively, Table 1. Since no structure was observed, the theoretical simulations were performed within the single mean phonon frequency approximation. For $S\omega_m \sim 200\,cm^{-1}$, the fits obtained with $S \sim 4$–6 and $\omega_m \sim 50$–$35\,cm^{-1}$ were quite satisfactory. It was suggested that if the special pair marker mode exists for P700, its frequency must be depressed relative to its values for P870 and P960. The fact that for P700 $S\omega_m \sim 200\,cm^{-1}$ is comparable to the optical reorganization energies for P870 and P960 (and about an order of magnitude greater than for antenna Chl) was taken as convincing evidence for P700 being a special pair and not a monomer.

C. Light harvesting complexes

Although X-ray structural data are sparse, biochemical and spectroscopic studies have provided valuable insights into the structure and organization of light harvesting complexes (LHC) within the antenna (Loach et al. 1985, Zuber 1985, Zuber et al. 1985, Breton et al. 1987). Energy transfer in antenna complexes have been the subject of recent reviews (van Grondelle 1985, Geacintov et al. 1987, Holzwarth 1989). A number of factors are important

for understanding the process that directs optical excitation into the RC. Included are the nature of the relevant excited states of chlorophylls (e.g., localized or delocalized), bath-induced mechanisms for homogeneous broadening of the pigment optical transitions and physical heterogeneity. One can anticipate, therefore, that under certain conditions the energy transfer processes may exhibit a significant temperature dependence.

(i) Antenna complex of Rb. sphaeroides

The antenna of *Rb. sphaeroides* is comprised of two main complexes, B800–B850 and B875, with the former peripheral to the latter, which surrounds and interconnects the RC. Various structural models have been proposed for B800–B850 (Kramer et al. 1984, Breton et al. 1987). It is generally accepted that the minimal structural subunit consists of two B850 and one B800 molecule, which are bound by two polypeptides (α and β). The polypeptides are approximately perpendicular to the membrane plane. The $\pi\pi^*$ Q_y-dipoles of the B850 molecules, attached to the α-helices, lie in the membrane plane, while the Q_x-dipoles are perpendicular. The B800 molecules have their Q_x- and Q_y-dipoles approximately parallel to the membrane plane. The center to center B850–B850 and B850–B800 distances have been estimated to be no greater than 15 and 21 Å, respectively (Bergstrom et al. 1986). The former distance is commensurate with an exciton coupling matrix element as large as about 100 cm^{-1} (Pearlstein 1988). It has been suggested, for example, that the above minimal subunit is the basis for a cyclic (C_n) 'unit cell' structure with $n \geq 3$.

Energy (singlet) transfer in the LHA has been extensively studied by picosecond techniques. The B850 to B875 transfer time is about 40 ps at room temperature (van Grondelle et al. 1987), whereas the B875 to RC (open) transfer time is about 60 ps (Freiberg et al. 1989) for chromatophores. The B800 to B850 transfer has been reported to be much faster, 2 ± 1 ps at 77 K (van Grondelle et al. 1987). More recently, experiments with femtosecond resolution have led to a transfer time of 2 ps at room temperature for the isolated B800–850 complex (Trautmann et al. 1990).

Non-photochemical hole burning of B800 established that the lifetime of B800* is 2.4 ps at pumped helium temperatures (van der Laan et al. 1990), which was shown to be due to energy transfer to B850 (Reddy et al. 1991b). Contrary to the findings of van der Laan et al. (1990), NPHB of B850 and B875 is as facile as for B800 (Reddy et al. 1991b). Hole burned spectra for the NFChr mutant (lacking in B875) is shown in Fig. 13. In spectra (a) and (b) a ZPH coincident with λ_B can be seen. The width of this hole is 4.2 ± 0.5 cm^{-1} implying a lifetime of 2.4 ± 0.2 ps for the B800 excited state. Within experimental uncertainty this value agrees with that determined by van der Laan et al. (1990). For λ_B within the B800 band the hole width is constant. In spectrum (b) the dominant BChl *a* vibration appears as a ZPH building on B800 origin ZPH at λ_B. Its frequency and FC factor are 750 cm^{-1} and 0.05, respectively. Features 1 and 2 in these spectra are the non-photochemical antihole and hole, respectively of the B850 band due to burning in B850* following its population by energy transfer. The features labeled by upward arrows can be confidently assigned as vibronic holes which build on the broad B850 hole. Spectrum

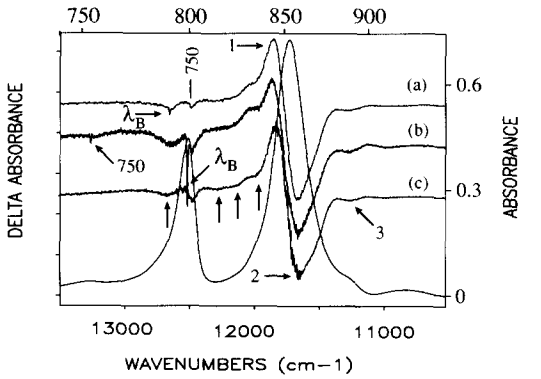

Fig. 13. Absorption and hole burned (Δ absorbance) spectra of mutant NFChr chromatophores of *Rb. sphaeroides*. Typical burn conditions for obtaining the hole burned spectra were 300 mW/cm^2 for 30 min. The read resolution is 2 cm^{-1}. Burn laser frequency is denoted by λ_B in spectra (a) and (b) and in spectrum (c) = 11 760 cm^{-1}. Hole marked 750 in (a) and (b) refer to the vibronic hole of the dominant intramolecular vibrational mode of BChl *a* building on B850 (a) and ZPH at (b), respectively. Feature 3 is the hole burned in the residual B875 band. Unlabelled vertical arrows refer to various vibronic holes building on the B850 hole. The upper horizontal scale gives the wavelength in nm and the right vertical axis refers to the absorption spectrum.

(c) of Fig. 13 is one of several obtained for λ_B located within B850. The broad ($210 \pm 20\,cm^{-1}$) B850 hole is very similar to those of spectra (a) and (b) and, furthermore, the width and peak position of the B850 hole are invariant to the location of λ_B within B850. This invariance means that Γ_H (minimum) for the B850 absorption band (width $280\,cm^{-1}$) is about $200\,cm^{-1}$ (Hayes et al. 1986, 1988, Reddy et al. 1991b). The origin of this large homogeneous broadening was identified from the observation that the $750\,cm^{-1}$ vibronic hole (width $60\,cm^{-1}$) which builds on the B850 hole is much narrower than $200\,cm^{-1}$. The only mechanism that can account for this novel vibronic hole narrowing effect is based on the well-known result that the exciton bandwidth of a vibronic transition is linearly proportional to its Franck–Condon factor (Craig et al. 1965, Hochstrasser 1966). Based on the data provided above, it follows that $\Gamma_H \approx 220\,cm^{-1}$ and $\Gamma_I = 60\,cm^{-1}$ for B850 and that $220\,cm^{-1}$ is a measure of the minimum exciton bandwidth for B850 (Reddy et al. 1991a).

In view of the finding that B850 is predominantly homogeneously broadened, with $\Gamma_H \sim 220\,cm^{-1}$ (due to exciton level structure and inter-exciton level scattering), it is not surprising that B800→B850 energy transfer is essentially temperature independent, *vide supra*. From Förster theory it follows that, if the donor and/or acceptor state carries a homogeneous broadening at liquid helium temperatures comparable to kT at room temperature, the energy transfer should be weakly temperature dependent. A bonus of the hole spectra given in Fig. 13 is that the dominant intramolecular modes in B800→B850 Förster transport are apparent, i.e., the $750\,cm^{-1}$ mode and $\sim 900\,cm^{-1}$ modes (left-most upward arrow) (Reddy et al. 1991b).

We have also studied the antenna of wild type *Rb. sphaeroides*, Fig. 14. Within experimental uncertainty, the lifetime of B800* is the same as for the mutant, as are the conclusions reached above for B850. Spectra (a) and (b) of Fig. 14 show that a broad B875 satellite hole results from excitation of either B800 or B850. Spectrum (c) was obtained by burning directly into B875 and, as was the case for the B850 hole, the broad B875 hole (width $210 \pm 20\,cm^{-1}$) was observed to be invariant to the location of λ_B within

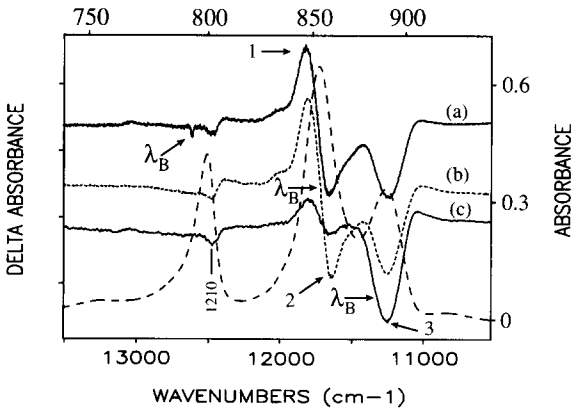

Fig. 14. Absorption and hole burned (Δ absorbance) spectra of wild type chromatophores of *Rb. sphaeroides*. Typical burn conditions are as in Fig. 13. Burn laser frequency for spectrum (c) is $11\,363\,cm^{-1}$. The read resolution is $4\,cm^{-1}$. Hole marked 1210 refers to the vibronic holes due to intramolecular vibrational modes of BChl *a* building on B850.

B875. The $1210\,cm^{-1}$ feature of spectrum (c) is a vibronic hole which builds on the B875 hole and is due to two closely spaced vibrations whose combined Franck–Condon factor is 0.05 (these and the above vibrational assignments are based, in part, on the high resolution vibronic excitation spectra of Renge et al. (1987)). The width of the $1210\,cm^{-1}$ vibronic hole is $80\,cm^{-1}$ and, in the manner briefly discussed for B850, the degree of vibronic hole narrowing can be used to determine that Γ_H for B875 is $\sim 200\,cm^{-1}$ (Reddy et al. 1991a). This homogeneous broadening is due predominantly to the excitonic mechanism discussed above for B850. That B850 and B875 should have similar excitonic bandwidths would be anticipated from structural models for the antenna (Kramer et al. 1984, Breton et al. 1987). Our results allow us to predict that B850→B875 energy transfer should be only weakly dependent on temperature.

(*ii*) *BChl* a *base plate antenna complex of* P. aestuarii

The water soluble BChl *a* complex from Prosthecochloris aestuarii, the Fenna–Matthews–Olson (FMO) complex, is one for which structural information is available (Mathews et al. 1980, Tronrud et al. 1986). The crystal structure revealed that the basic structural unit is a trimer of subunits, each containing seven BChl *a* mole-

cules which are not symmetry equivalent. Nearest neighbor Mg..Mg distances within a subunit vary between 11.3 and 14.4 Å while the edge-to-edge distances between subunits (within a given trimer) are ≈25 Å. The complex is devoid of the RC. Furthermore, the relative orientations of the BChl *a* molecules within the subunit are not appropriate for the formation of 'dark' intermolecular charge-transfer states which might mediate energy transfer between the 'light' Q_y-states. Pairwise dipole-dipole matrix elements within the subunit are as large as $\approx 200\,cm^{-1}$ (Mathews et al. 1980, Pearlstein 1988). The weakest interactions between BChl monomers in a given subunit are $\approx 10\,cm^{-1}$, which is comparable to the strongest interaction between monomers of different subunits of the trimer.

The 4.2 K absorption spectrum of the FMO complex in a glass is shown in Fig. 15 and exhibits five discernible components at 825, 814, 805, 800 and 794 nm (none of which can be reasonably assigned to vibrational structure). Although this structure and the CD spectra cannot be understood in the absence of excitonic interactions, attempts to do so in terms of a single subunit have not been successful (Pearlstein 1978, Mathews et al. 1980). One difficulty has been the prediction of the absorption band at 825 nm as well as its CD signature. It has been suggested that this difficulty cannot be resolved by allowing for diagonal energy disorder of the 7 BChl *a* (Pearlstein, private communication). Such disorder is mandated by the X-ray structure which shows conformational variations between the BChl *a* monomers as well as significant difference in axial ligand binding to Mg. Indeed, recent quantum chemical calculations by Gudowska-Nowak et al. (1990) indicate that the diagonal energy disorder for the Q_y-states is greater than the observed width of the Q_y-absorption region ($\approx 500\,cm^{-1}$). Although these calculations overestimate the diagonal energy disorder, they indicate that this disorder should be treated on an equal footing with the excitonic interactions.

Following our first report on the NPHB of the FMO complex (Johnson et al. 1989), a far more detailed paper appeared (Johnson et al. 1991a). Only a few of the persistent NPHB spectra are presented and discussed here. Before doing so, we provide the most important findings: A minimum of eight (not seven as expected for the single subunit model) states contribute to the Q_y-absorption spectrum of Fig. 15, with two states contributing to the 824 nm absorption band, cf. Table 2; the hole spectra are consistent with a connectivity between the states which is expected for states that are delocalized due to

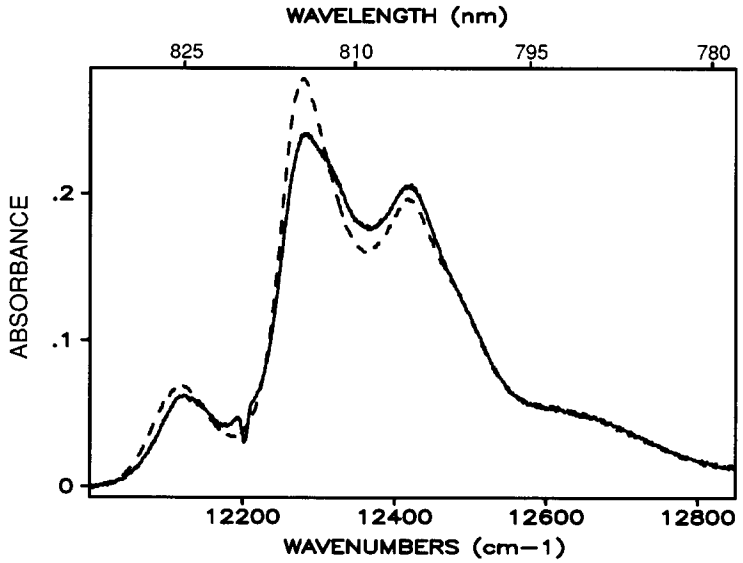

Fig. 15. Preburn absorption spectrum (dashed line) and hole-burned absorption spectrum (solid line) of *P. aestuorii* for $\lambda_B = 819.5$ nm. These spectra provide the ΔA spectrum for Fig. 17C. See Fig. 17 caption for details.

Table 2. Exciton components

Component	Wavelength (nm)/(cm^{-1})	Excited state decay time[a]
1	827.1 (12 090)	≥20. ps[b]
2	824.4 (12 130)	≥20. ps
3	816.3 (12 250)	100 fs[c]
4	813.0 (12 300)	100 fs
5	807.8 (12 380)	100 fs
6	804.8 (12 425)	100 fs
7	801.3 (12 480)	100 fs
8	793.6 (12 600)	100 fs

[a] Decay time of exciton state as measured by burning directly into that state.
[b] Holewidth 0.5 cm^{-1} for components 1 and 2.
[c] Holewidth 50 cm^{-1} for components 3–8.

strong excitonic interactions; the results are most consistent with excited state electronic structure from a trimer of subunits; the CD spectra may well depend sensitively on the relatively weak excitonic interactions between the subunits of the trimer; and inter-exciton level 'Davydov' scattering, from the upper exciton levels occurs in ~100 fs, cf. Table 2. Subsequently, Pearlstein has found that the trimer of subunits model leads to a significant improvement between the calculated and experimental CD spectra (private communication). Thus, it appears that a minimum of 21 BChl *a* molecules are required for an adequate description of the excited state structure. To a first approximation, the C_3-symmetry axis of the trimer leads to the 14 states polarized perpendicular to the C_3-axis occurring in doubly degenerate pairs, while the other 7 states, polarized parallel to C_3, are non-degenerate. An important point for theoretical studies is that inherent statistical structural fluctuations from subunit to subunit may significantly perturb the apparent 3-fold screw-axis symmetry of the trimer.

The solid spectrum (Fig. 15) is the absorption following a burn at the position of the arrow, which is coincident with the ZPH (the ΔA hole burned spectrum is given as trace *c* in Fig. 16). The two most striking aspects of the spectra in Fig. 15 are: The significant blue-shifting of the entire absorption spectrum and intensity redistribution produced by hole burning; and that the absorption features to higher energy of λ_B (as well as lower) are affected. Noting that at 4.2 K only downward energy transfer from the burn frequency is possible, it is immediately apparent

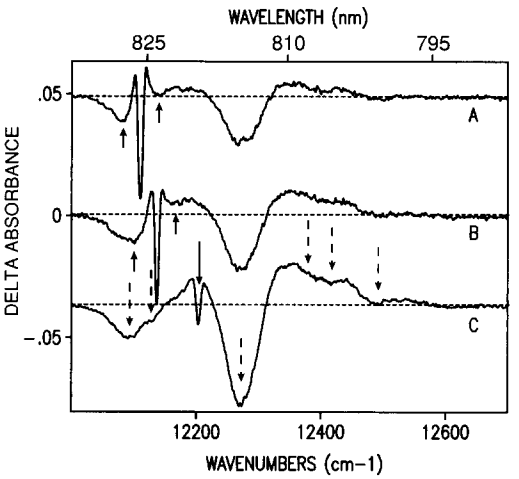

Fig. 16. Hole spectra of *P. aestuorii*, λ_B = (A) 825.5 nm (12 114 cm^{-1}), (B) 823.5 nm (12 143 cm^{-1}), and (C) 819.5 nm (12 202 cm^{-1}). Burn intensities: (A) 150 mW/cm^2, (B) 230 mW/cm^2, and (C) 400 mW/cm^2. Burn times: (A) 7 min, 40 s; (B) 8 min, 15 s; and (C) 6 min, 15 s. Solid arrows pointing downwards indicate λ_B while those pointing upward indicate real- and pseudo-PSBH. Dashed arrows indicate satellite holes. Dashed horizontal lines indicate ΔA = 0. T = 4.2 K and read resolution 2 cm^{-1}. Same vertical scale applies to each spectrum (spectra A and C offset for clarity).

that these observations cannot be understood in the absence of connectivity between the different absorption bands (states).

The hole spectra in Fig. 16 labeled as A, B and C correspond to λ_B = 825.5, 823.5 and 819.5 nm, respectively. The sharp ZPH at λ_B in A and B correspond to a 70% OD change. According to theory (Hayes et al. 1986), the fractional OD change for the saturated ZPH is given by exp(−S), where S is the Huang–Rhys factor for the protein phonons. A OD change of 70% corresponds to an S-value of 0.3. This value is nearly a factor of 3 smaller than observed for Chl *a* in the light harvesting complex of photosystem I of spinach (Gillie et al. 1989b) and represents the weakest linear electron-phonon coupling observed to date for antenna complexes. The phonons to which the transition electron couples are responsible for the relatively broad phonon-sideband holes (PSBH) which appear at $\omega_m \approx 30\ cm^{-1}$ to higher and lower energy of the ZPH in spectrum (A) of Fig. 16. Focusing first on the pseudo-PSBH at $-30\ cm^{-1}$ we observe that its shape in spectrum (B) is distorted (fattened). This distortion cannot be explained by

linear electron-phonon coupling. Rather, it is most likely a manifestation of energy transfer from the isochromat excited at λ_B to lower energy absorbers of the 825 nm absorption band. This interpretation is supported by the fluorescence spectra of this complex (Johnson et al. 1991a). Downward energy transfer is inconsistent with the interpretation that views the 825 nm band as being due to a single state of a 7 BChl *a* containing subunit. Spectrum (C) of Fig. 16 provides additional support for energy transfer. It was obtained with $\lambda_B = 819.5$ nm (12 202 cm^{-1}), located in the valley between the 825 and 814 nm absorption bands. Two holes, indicated by dashed arrows, are observed at 828 and 824 nm. They are denoted as components 1 and 2 in Table 2. It is important to note that the centroid of the overall hole profile is close to 828 nm and not 825 nm, which is the maximum of the lowest energy absorption band, Fig. 15. All three spectra exhibit a prominent higher energy satellite hole at 814 nm. However, spectra obtained for λ_B located in the low energy side of the 825 nm band revealed that the 814 nm hole is a doublet with components at 816 and 813 nm, see Table 2.

Figure 17 shows the NPHB spectrum obtained with $\lambda_B = 800.0$ nm (solid arrow). Seven of the eight states (located by arrows) listed in Table 2

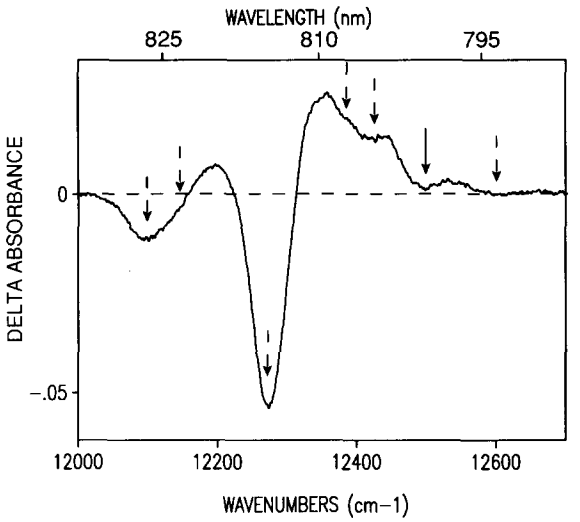

Fig. 17. Hole spectra of *P. aestuorii*, $\lambda_B = 800.0$ nm (12 500 cm^{-1}). Burn intensity of 800 mw/cm^2. Burn time of 1 min, 30 s. Arrows, *T*, read resolution and horizontal lines same as in Fig. 17.

are visible. It is apparent that the intensity distribution is determined, in part, by the interplay between the hole and anti-hole profiles. For example, in Fig. 17 the four highest energy holes are obviously superimposed on an anti-hole derived mainly from the most intense hole at 814 nm.

The decay times for the eight exciton states given in Table 2 were determined by burning directly into these states. For states 5–8 this was complicated by the interference generated by the broad anti-hole associated with the 814 nm hole. The hole widths of components 3–8 were essentially identical (±20%) and are stated as 50 cm^{-1}, corresponding to an energy transfer decay time of 100 fs. The lowest energy states, components 1 and 2, yielded hole widths of 0.5 cm^{-1} which correspond to excited state decay times of 20 ps. As discussed by Johnson et al. (1991a), the hole width for component 1 (827.1 nm state) does not represent lifetime (T_1) broadening. The average level spacing for the observed exciton states is ~50–75 cm^{-1} with two exceptions. There are two larger gaps in the exciton manifold of ~125 cm^{-1}, between the 824.4 and 816.3 nm states and between 801.3 and 793.36 nm states. However, for the trimer of subunits model there are 14 states, seven of which are doubly degenerate. With the interpretation that the 827.1/824.4 nm states correspond to the parallel and perpendicular components of the trimer derived from a single subunit exciton state, it is reasonable to suggest that the higher energy absorption bands are also contributed to by unresolvable parallel and perpendicular components (we cannot prove or disprove that the 816/813 or 808/805 cm^{-1} states are such component pairs). In addition, one expects that (Pearlstein 1988, private communication) ≈2–3 of the subunit exciton states would be weakly absorbing and that the corresponding trimer states are too weak to have been detected. The point is that the level spacing could be significantly denser than indicated by Table 2.

Although 'dark' states are not expected to be important for Förster energy transfer, Förster theory is not applicable to a strongly exciton coupled system like the FMO complex since the states excited are delocalized and, therefore, diagonal with respect to the intermolecular poten-

tial energy, V_{int}. It is V_{int} that enters into the Fermi-Golden rule expression for Förster transfer. For the FMO complex, inter-exciton level scattering (relaxation) must be induced by $(\partial V_{int}/\partial Q)_0 Q$ (and possibly higher order terms) and described by Davydov theory (Davydov 1971). Here Q is a suitable intermolecular mode(s) which modulates the pair-wise excitonic interactions. Hindered rotational (librational) motions of the BChl molecules about axes perpendicular to the Q_y-transition dipole are expected to be most effective (Dissado 1975).

IV. Future Prospects

There are several new types of hole burning experiments which can be suggested for future studies of antenna and reaction center complexes: although some polarized (linear dichroism) hole burning experiments have been performed, they should receive greater attention since the additional spectral resolution afforded by hole burning together with polarization anisotropy should lead to an improved understanding of the excited electronic states of coupled pigment aggregates; Stark experiments in which the zero-phonon hole is studied can provide a direct and high resolution approach to dipole moment and polarizability changes which accompany electronic excitation; and pressure-dependent studies of the zero-phonon hole as well as the entire hole spectrum would yield information on the pressure dependence of energy gaps, excited state lifetimes and the compressibility of proteins.

Acknowledgments

Ames Laboratory is operated for the U.S. Department of Energy by Iowa State University under Contract No. W-7405-Eng-82. This research was supported by the Division of Chemical Sciences, Office of Basic Energy Sciences, U.S. Department of Energy. P.A.L. is most grateful to William Catron for his graduate student fellowship. Our work discussed in this review would not have been possible without the active collaborations developed with J. Golbeck, D. Tiede, M. Seibert, R. Picorel, C. Yocum, T. Dimagno and J. Norris. We thank C. Yocum and T. Dimagno and J. Norris for permission to present some of our unpublished results on the CP-47-D1–D2–Cyt *b* 559 complex and the fully deuterated RC of *Rb. sphaeroides*. Full reports on these projects are forthcoming. The cofactor structure for the RC of *Rb. sphaeroides* was kindly provided by D. Tiede.

References

Allen JP, Feher G Yeates TO, Rees DC, Deisenhofer J, Michel H and Huber R (1986) Structural homology of reaction centers from *Rhodopseudomonas sphaeroides* and *Rhodopseudomonas viridis* as determined by X-ray diffraction. Proc Natl Acad Sci (USA) 83: 8589–8593

Allen JP, Feher G Yeates TO, Komiya H and Rees DC (1987) Structure of the reaction center from *Rhodobacter sphaeroides* R-26: The cofactors. Proc Natl Acad Sci (USA) 84: 5730–5734

Beckman RL, Hayes JM and Small GJ (1977) Neat and mixed crystal and glass optical spectra of the Anthracene-Trinitrobenzene complex. Chem Phys 21: 135–144

Berg M, Walsh CA, Narasimhan LR, Littau KA and Fayer MD (1988) Dynamics in low temperature glasses: theory and experiments on optical dephasing, spectral diffusion, and hydrogen tunneling. J Chem Phys 88: 1564–1587

Bergstrom H, Sundstrom V, van Grondelle R, Akesson E and Gillbro T (1986) Energy transfer within the isolated light-harvesting B800–850 pigment-protein complex of *Rhodobacter sphaeroides*. Biochim Biophys Acta 852: 279–287

Bergstrom H, Sundstrom V, van Grondelle R, Gillbro T and Cogdell RJ (1988) Energy transfer dynamics of isolated B800–850 and B800–820 pigment protein complexes of *Rhodobacter sphaeroides* and *Rhodopseudomonas acidophila*. Biochim Biophys Acta 936: 90–98

Bixon M and Jortner J (1982) Quantum effects on electron-transfer processes. Faraday Discuss Chem Soc 74: 17–29

Bixon M and Jortner J (1989) Activationless and pseudo-activationless primary electron transfer in photosynthetic bacterial reaction centers. Chem Phys Lett 159: 17–20

Boxer SG, Lockhart DJ and Middendorf TR (1986a) Photochemical holeburning in photosynthetic reaction centers. Chem Phys Lett 123: 476–482

Boxer SG, Middendorf TR and Lockhart DJ (1986b) Reversible photochemical holeburning in *Rhodopseudomonas viridis* reaction centers. FEBS Lett 200: 237–241

Breton J and Nabedryk E (1987) Pigment and protein organization in reaction centers and Antenna complexes. In: Barber J (ed) The Light Reactions, pp 159–195. Amsterdam: Elsevier

Breton J, Martin J-L, Fleming GR and Lambry J-C (1988a) Low temperature femtosecond spectroscopy of the initial

step of electron transfer in reaction centers from photosynthetic bacteria. Biochem 27: 8276–8284

Breton J and Vermeglio A (eds) (1988b) The Photosynthetic Bacterial Reaction Center. New York: Plenum Press

Chang CH, Tiede DM, Tang J, Smith U, Norris J and Schiffer M (1986) Structure of *Rhodopseudomonas sphaeroides* R-26 reaction center. FEBS Lett 205: 82–86

Clayton RK and Sistrom WR (eds) (1971) The Photosynthetic Bacteria. New York: Plenum Press

Craig DP and Gordon RD (1965) The crystal structure of phenanthrene and phenanthrene-d_{10} near 3400 A. Proc R Soc (London) A 288: 69–97

Davydov AS (1971) Theory of Molecular Excitons. New York: Plenum Press

Deisenhofer J, Epp O, Miki K, Huber R and Michel H (1984) X-ray structure analysis of a membrane protein complex. Electron density map at 3 Å resolution and a model of the chromophores of the photosynthetic reaction centers from *Rhodopseudomonas viridis*. J Mol Biol 180: 385–398

Deisenhofer J, Epp O, Miki K, Huber R and Michel H (1985) Structure of Protein subunits in the photosynthetic reaction center of *Rhodopseudomonas viridis* at 3 Å resolution. Nature (London) 318: 618–624

Dekker JP, Bowlby NR and Yocum CY (1989) Chlorophyll and cytochrome *b*-559 content of the photochemical reaction center of Photosystem II. FEBS Lett 254: 150–154

Dissado LA (1975) Linewidths of the 3800 A singlet transitions in crystalline anthracene. Chem Phys 8: 289–303

Donohoe RJ, Dyer RB, Swanson BI, Violette CA, Frank HA and Bocian DF (1990). J Am Chem Soc 112: 6716–6718

Fleming GR, Martin J-L and Breton J (1988) Rates of primary electron transfer in photosynthetic reaction centers and their mechanistic implications. Nature 333: 190–192

Freiberg A, Godik VI, Pullerits T and Timpmann K (1988) Directed picosecond excitation transport in purple photosynthetic bacteria. Chem Phys 128: 227–235

Freiberg A, Godik VI, Pullerits T and Timpmann K (1989) Picosecond dynamics of directed excitation transfer in spectrally heterogeneous light-harvesting antenna of purple bacteria. Biochim Biophys Acta 973: 93–104

Friedrich J and Haarer D (1984) Photochemical hole burning: A spectroscopic study of relaxation processes in polymers and glasses. Angew Chem Int Engl Ed 23: 113–140

Friesner RA and Won Y (1989a) Spectroscopy and electron transfer dynamics of the bacterial photosynthetic reaction centers. Biochim Biophys Acta 977: 99–122

Friesner RA and Won Y (1989b) Photochemical charge separation in photosynthetic reaction centers. Photochem Photobiol 50: 831–839

Geacintov NE and Breton J (1987) Energy transfer and fluorescence mechanism in photosynthetic membranes. In: Congor BV (ed) Critical Reviews in Plant Science, Vol 5, pp 1–44. Boca Raton: CRC Press

Ghanotakis DF, de Paula PC, Demetrou DM, Bowlby NR, Petersen J, Babcock GJ and Yocum CF (1989) Isolation and characterization of the 47 kDa protein and the D1–D2–cytochrome *b*-559 complex. Biochim. Biophys. Acta 974: 44–53

Gillie JK, Lyle PA and Small GJ (1989a) Spectral hole burning of the primary electron donor state of photosystem I. Photosynth Res 22: 233–246

Gillie JK, Small GJ and Golbeck JH (1989b) Nonphotochemical holeburning of the native complex of Photosystem I (PS I-200). J Phys Chem 93: 1620–1627

Govindjee (ed) (1975) Bioenergetics of Photosynthesis. New York: Academic Press

Gudowska-Nowak E, Newton MD and Fajer J (1990) Conformational and environmental effects of Bacteriochlorophyll optical spectra: Correlations of calculated spectra with structural results. J Phys Chem (1990), submitted for publication

Haarer D (1974) Zero-phonon transitions and vibronic coupling in the 1:1 charge-transfer crystal Anthracene-pyromellitic acid-dianhydride. Chem Phys Lett 27: 91–95

Haarer D (1987) Photochemical hole-burning in electronic transition. In: Moerner WE (ed) Topics in Current Physics, Persistent Spectral Hole Burning: Science and Applications, pp 79–123. New York: Springer-Verlag

Hayes JM and Small GJ (1978) Non-photochemical hole burning and impurity site relaxation processes in organic glasses, Chem Phys 27: 151–157

Hayes JM and Small GJ (1986) Photochemical hole burning and strong electron phonon coupling: primary donor states of reaction centers of photosynthetic bacteria. J Phys Chem 90: 4928–4931

Hayes JM, Jankowiak R and Small GJ (1987) Two-level system relaxation in amorphous solids as probed by nonphotochemical hole-burning in electronic transitions. In: Moerner WE (ed) Topics in Current Physics, Persistent Spectral Hole Burning: Science and Applications, Vol 44, pp 153–202. New York: Springer-Verlag (and references therein)

Hayes JM, Gillie JK, Tang D and Small GJ (1988) Theory for spectral hole burning of the primary electron donor state of photosynthetic reaction centers. Biochim Biophys Acta 932: 287–305

Hochstrasser RM (1966) Molecular Aspects of Symmetry. New York: Benjamin WA, Inc

Holzapfel W, Finkele U, Kaiser W, Oesterhelt D, Scheer H, Stilz HU and Zinth W (1990) Initial electron transfer in the reaction center from *Rhodobacter sphaeroides*. Proc Natl Acad Sci (USA) 87: 5168–5172

Holzwarth AR (1989) Applications of ultrafast laser spectroscopy for the study of biological systems. Quart Rev Biophys 22: 239–326

Huber DL, Broer MM and Golding (1984) Low-temperature optical dephasing of rare-earth ions in glass. Phys Rev B 52: 2281–2284

Hunter CN, van Grondelle and Olsen JD (1989) Photosynthetic antenna proteins: 100 ps before photochemistry starts. Trends Biochem Sci 14: 72–76

Jankowiak R, Shu L, Kenney M and Small GJ (1987a) Dispersive kinetic processes, optical linewidths and dephasing in amorphous solids. J Lumin 36: 293–305

Jankowiak R and Small GJ (1987b) Hole-burning spectroscopy and relaxation dynamics of amorphous solids at low temperatures. Science 237: 618–625

Jankowiak R, Tang D and Small GJ (1989) Transient and persistent hole-burning of the reaction center of Photosystem II. J Phys Chem 93: 1649–1654

Johnson SG and Small GJ (1989a) Spectral hole burning of a strongly exciton coupled Bacteriochlorophyll *a* antenna complex. Chem Phys Lett 155: 371–375

Johnson SG, Tang D, Jankowiak, R, Hayes JM and Small GJ (1989b) Spectral hole burning: A window on energy transfer in photosynthetic units. In: Fiala J and Pokorny J (eds) Proceedings of VIth International conference on Energy and Electron Transfer Prague: Charles University

Johnson SG, Tang D, Jankowiak R, Hayes JM, Small GJ and Tiede DM (1989c) Structure and marker mode of the primary electron donor state absorption of photosynthetic bacteria: Hole-burned spectra. J Phys Chem 93: 5953–5957

Johnson SG, Tang D, Jankowiak R, Hayes JM, Small GJ and Tiede DM (1990) Primary donor state mode structure and energy transfer in bacterial reaction centers. J Phys Chem 94: 5849–5855

Johnson SG and Small GJ (1991a) Excited state structure and energy transfer dynamics of the Bacteriochlorophyll *a* antenna complex form Prosthecochloris aestuarii. J Phys Chem 95: 471–479

Johnson SG, Lee I-J and Small GJ (1991b) Solid state spectral line narrowing spectroscopies in: Scheer H (ed) Chlorophylls, pp 739–768. CRC Press, Boca Raton

Jortner J (1980) Dynamics of electron transfer in bacterial photosynthesis. Biochim Biophys Acta 594: 193–230

Jortner J and Pullman B (eds) (1990) Perspectives in Photosynthesis. Dordrecht: Kluwer Academic Press

Kenney MJ, Jankowiak RJ and Small GJ (1990) Dispersive kinetics of nonphotochemical hole growth for Oxazine 720 in glycerol, polyvinyl alcohol and their deuterated analogues. Chem Phys 146: 47–61

Kirmaier C and Holten D (1987) Primary photochemistry of reaction centers from the photosynthetic purple bacteria. Photosynth Res 13: 225–260

Kirmaier C, Holten D and Parson WW (1985) Temperature and detection-wavelength dependence of the picosecond electron transfer kinetics measured in *Rhodopseudomonas sphaeroides* reaction centers. Resolution of new spectral and kinetic components in primary charge separation processes. Biochim Biophys Acta 810: 33–48

Knox RS (1986) Trapping events in light-harvesting assemblies, In: Staehelin LA and Arntzen CJ (eds) Encyclopedia of Plant Physiology, Vol 19, pp 286–298. Springer-Verlag, Berlin

Kobayashi M, Maeda H, Watanabe T, Nakane H and Satoh K (1990) Chlorophyll *a* and β-carotene content in the d_1/d_2/cytochrome *b*-559 reaction center complex from spinach. FEBS Lett 260: 138–140

Kramer HJM, van Grondelle R, Hunter CM, Westerhuis WHJ and Amesz J (1984) Pigment organization of the B800–850 antenna complex of *Rhodobacter sphaeroides*. Biochim Biophys Acta 765: 156–165

Lee I-J, Hayes JM and Small GJ (1989) Hole and anti-hole profiles in nonphotochemical holeburned spectra. J Chem Phys 91: 3463–3469

Levenson MD and Kano S (1988) Introduction to nonlinear laser spectroscopy (Quantum Electronics – Principles and Applications). Boston: Academic Press

Loach PA, Parkes PS, Miller JF, Hinchigeri S and Callahan PM (1985) Structure-function relationships of the bacteriochlorophyll-protein light-harvesting complex of *Rhodospirillum rubrum*, In: Steinback KE, Bonitz S, Arntzen CJ and Bogorad L (eds) Molecular Biology of the Photosynthetic Apparatus, pp 197–209. Cold Spring Harbor Laboratory, New York

Lockhart DJ and Boxer SG (1988) Stark effect spectroscopy of *Rhodobacter sphaeroides* and *Rhodopseudomonas viridis* reaction centers. Proc Nat Acad Sci (USA) 85: 107–111

Lockhart DJ, Kirmaier C, Holten D and Boxer SG (1990) Electric field effects on the initial electron transfer kinetics in bacterial photosynthetic reaction centers. J Phys Chem 94: 6987–6995

Lösche M, Feher G and Okamura MY (1987) The Stark effect in reaction centers from *Rhodobacter sphaeroides* R-26 and *Rhodopseudomonas viridis*. Proc Nat Acad Sci (USA) 84: 7537–7541

Lösche M, Feher G and Okamura MY (1988) The Stark effect in photosynthetic reaction centers from *Rhodobacter sphaeroides* R-26, *Rhodopseudomonas viridis* and the D_1D_2 complex of Photosystem II from spinach. In: Breton J and Vermeglis A (eds) The Photosynthetic Bacterial Reaction Center: Structure and Dynamics, pp 151–164. Plenum Press, New York

Lyle PA and Small GJ (1991) unpublished results

Lyo SK (1986) Dynamical theory of optical linewidths in glasses. In: Zschokke I (ed) Optical Spectroscopy of Glasses, pp 1–21 (and references therein)

Matthews BW and Fenna RE (1980) Structure of a green bacteriochlorophyll protein. Acc Chem Res 13: 309–317

Matthews BW, Fenna RE, Bolognesi MC, Schmid MF and Olson JM (1979) Structure of Bacteriochlorophyll *a*-protein from the green photosynthetic bacterium Prosthecochloris aestuarii. J Mol Biol 131: 259–285

McTavish H, Picorel R and Seibert M (1989) Stabilization of isolated PS II reaction complex in the dark and in the light using polyethylene glycol. Plant Physiol 98: 452–456

Meech SR, Hoff AJ and Wiersma DA (1985) Evidence for a very early intermediate in bacterial photosynthesis: A photon echo and holeburning study of the primary donor band in *Rhodopseudomonas sphaeroides*. Chem Phys Lett 121: 287–292

Michel-Beyerle ME (ed) (1985) Antennas and Reaction Centers of Photosynthetic Bacteria. Springer-Verlag: Berlin

Michel H and Deisenhofer J (1986a) X-ray diffraction studies on a crystalline bacterial photosynthetic reaction center. A progress report and conclusions on the structure of Photosystem II reaction centers. In: Staehelin AC and Arntzen CJ (eds) Encyclopedia of Plant Physiology: Photosynthesis III pp 371–381. Springer Verlag, Berlin

Michel H, Epp O and Deisenhofer J (1986b) Pigment-protein interactions in the photosynthetic reaction center from *Rhodopseudomonas viridis*. EMBO J 5: 2445–2451

Moerner WE (ed) (1987) Topics in Current Physics, Persistent Spectral Hole Burning: Science and Applications, Vol 44. Springer-Verlag, New York

Nanba O and Satoh K (1987) Isolation of a Photosystem II reaction center consisting of D-1 and D-2 polypeptides and cytochrome *b*-559. Proc Natl Acad Sci (USA) 84: 109–112

Narasimhan LR, Littau KA, Pack DW, Bai YS, Elschner A and Fayer MD (1990) Probing organic glasses at low temperature with variable time scale optical dephasing experiments. Chem Rev 90: 439–457

Norris JR and Schiffer M (1990) Photosynthetic reaction centers in bacteria. Chem Engr News 68: 22–37

Ogrodnik A, Ebert U, Heckmann R, Kappl M, Feick R and Michel-Beyerle ME (1991) Excitation dichroism of electric field modulated fluorescence yield for the identification of primary electron acceptor in photosynthetic reaction center. J Phys Chem 95: 2036–2041

Okamura MY, Satoh K, Issacson RA and Feher G (1986) Evidence for primary charge separation in D_1D_2 complex of Photosystem II from spinach: EPR of the triplet state. In: Biggins J (ed) Progress in Photosynthesis Research, Vol I, pp 379–381. Martius Nijhoff, Boston

Pearlstein RM (1982) Chlorophyll singlet excitons. In: Govindjee (ed) Photosynthesis: Energy Conversion by Plants and Bacteria, pp 293–330. Academic Press, New York

Pearlstein RM (1988) In: Scheer H and Schneider S (eds) Photosynthetic Light Harvesting Systems, pp 555. De Gruyter, Berlin

Pearlstein RM and Hemenger RP (1978) Bacteriochlorophyll electronic transition moment directions in Bacteriochlorophyll *a*-protein. Proc Natl Acad Sci USA 75: 4920–4924

Pearlstein RM and Zuber H (1985) Exciton state and energy transfer in bacterial membranes: The role of pigment-protein cyclic unit structures. In: Michel-Beyerle ME (ed) Springer Series in Chemical Physics 42: Antennas and Reaction Centers of Photosynthetic Bacteria, ed. pp 53–61. Springer-Verlag, Berlin

Port H, Rund D, Small GJ and Yakhot V (1979) The exciton-phonon interaction for triplet exciton bands of organic solids: An experimental and theoretical study. Chem Phys 39: 175–188

Reddy NRS and Small GJ (1991) Hole burning as a probe of exciton bandwidths in amorphous solids. J Chem Phys 94: 7545–7546

Reddy NRS, Small GJ, Seibert M and Picorel R (1991) Energy transfer dynamics of the B800–B850 antenna complex of *Rhodobacter sphaeroides*: A hole burning study. Chem Phys Letts 181: 391–399

Renge I, Mauring K and Avarmaa R (1987) Site-selection optical spectra of bacteriochlorophyll and bacteriopheophytin in frozen solution. J Lumn 37: 207–214

Robinette SC, Small GJ and Stevenson SH (1978) An optical study of the temperature dependent scattering of the *a* exciton (polariton) of naphthalene. J Chem Phys 68: 4790–4803

Sargeant III M, Scully MO and Lamb Jr WE (1974) Laser Physics. Addison-Wesley, Reading

Scherer POJ and Fischer S (1989) Long-range electron transfer within the hexamer of the photosynthetic reaction center, *Rhodopseudomonas viridis* 93: 1633–1637

Shu L and Small GJ (1990) On the mechanism of non-photochemical hole burning of optical transitions in amorphous solids. Chem Phys 141: 447–455

Tang D, Jankowiak R, Small GJ and Tiede DM (1989) Structured hole burned spectra of the primary donor state absorption region of *Rhodopseudomonas viridis*. Chem Phys 131: 99–113

Tang D, Jankowiak R, Seibert M and Small GJ (1990a) Effects of detergent on the excited state structure and relaxation dynamics of the Photosystem II reaction center: A high resolution hole burning study. Photosynth Res 27: 19–29

Tang D, SG, Jankowiak R, Hayes JM, Small GJ and Tiede DM (1990b) Structure and marker mode of the primary electron donor state absorption of photosynthetic bacteria: Hole-burned spectra. In: Jortner J and Pullman B (eds) Twenty Second Jerusalem Symposium Quantum chemistry and Biochemistry: Perspectives in Photosynthesis, pp 99–120. Kluwer Academic Publishers, Dordrecht

Tang D, Jankowiak R, Seibert M, Yocum CF and Small GJ (1990c) Excited-state structure and energy-transfer dynamics of two different preparations of the reaction center of Photosystem II: A hole burning study. J Phys Chem 94: 6519–6522

Trautmann JK, Shreve AP, Violette CA, Frank HA, Owens TG and Albrecht AC (1990) Femtosecond dynamics of energy transfer in B800–850 light harvesting complexes of *Rhodobacter sphaeroides*. Proc Natl Acad Sci USA 87: 215–219

Tronrud DE, Schmid MF, Matthews BW (1986) Structure and X-ray amino acid sequence of a bacteriochlorophyll *a* protein from Prosthecochloris aestuarii refined at 1.9 Å resolution. J Mol Biol 188: 443–454

van der Laan H, Schmidt Th, Visschers RW, Visscher KJ, van Grondelle R and Volker S (1990) Energy transfer in B800–850 complex of purple bacteria *Rhodobacter sphaeroides*: a study by spectral hole burning. Chem Phys Letts 170: 231–238

van Grondelle R (1985) Excitation energy transfer, trapping and annihilation in photosynthetic systems. Biochim Biophys Acta 811: 147–195

van Grondelle R, Bergstrom H, Sundstrom V and Gillbro T (1987) Energy transfer within the Bacteriochlorophyll antenna of purple bacteria at 77 K, studied by picosecond absorption recovery. Biochim Biophys Acta 894: 313–326

Vermeglio A and Paillotin G (1982) Structure of *Rhodopseudomonas viridis* reaction centers. Absorption and photoselection at low temperature. Biochim Biophys Acta 681: 32–40

Völker S (1989) Structured hole-burning in crystalline and amorphous organic solids. In: Funfschilling J (ed) Molecular Excited States, Optical relaxation processes at low temperatures, pp 113–242. Kluwer Academic Publishers, Dordrecht

Walsh CA, Berg M, Narasimhan LR and Fayer MD (1986) Optical dephasing of chromophores in an organic glass:

Picosecond photon echo and hole burning experiments. Chem Phys Lett 130: 6–11

Walsh CA, Berg M, Narasimhan LR and Fayer MD (1987a) Probing intermolecular interactions with picosecond photon echo experiments. Accounts Chem Res 20: 120–126

Walsh CA, Berg M, Narasimhan LR and Fayer MD (1987b) A picosecond photon echo study of a chromophore in an organic glass: Temperature dependence and comparison to non-photochemical holeburning. J Chem Phys 86: 77–87

Warshel A and Parson WW (1987) Spectroscopic properties of photosynthetic reaction centers I. Theory. J Am Chem Soc 109: 6143–6152

Wasielewski MR, DG, Govindjee, Preston C and Seibert M (1989a) Determination of the primary charge separation rate in photosynthetic reaction center at 15 K. Photosynth Res 22: 89–99

Wasielewski MR, Johnson DG, Seibert M and Govindjee (1989b) Determination of the primary charge separation rate in isolated Photosystem II reaction centers with 500 fs time resolution. Proc Natl Acad Sci (USA) 86: 524–528

Whitten WB, Olson JM, Pearlstein RM (1980) Seven-fold exciton splitting of the 810-nm band in Bacteriochlorophyll *a*-proteins from green photosynthetic bacteria. Biochim Biophys Acta 591: 203–207

Won Y and Friesner RA (1987) Simulation of photochemical hole-burning experiments on photosynthetic reaction centers. J Proc Natl Acad Sci (USA) 84: 5511–5515

Won Y and Friesner RA (1988a) Theoretical studies of photochemical holeburning in photosynthetic reaction centers. J Phys Chem 92: 2214–2219

Won Y and Friesner RA (Comment) (1988b) Theoretical studies of photochemical holeburning in bacterial reaction centers. J Phys Chem 93: 1007

Yeates TO, Komiya H, Chirino A, Rees DC, Allen JP and Feher G (1988) Structure of the reaction center from *Rhodobacter sphaeroides* R-26 and 2.4.1: Protein-cofactor (bacteriochlorophyll, bacteriopheophytin and carotenoid) interactions. Proc Natl Acad Sci (USA) 85: 7993–7997

Zuber H (1985a) Structure and function of light-harvesting complexes and their polypeptides. Photochem Photobiol 42: 821–844

Zuber H, Sidler W, Füglistaller P, Brunisholz R and Theiler R (1985b) Structural studies on the light-harvesting polypeptides from Cyanobacteria and Bacteria. In: Steinback KE, Bonitz S, Arntzen CJ and Bogorad L (eds) Molecular Biology of the Photosynthetic Apparatus, pp 183–195. Cold Spring Harbor Laboratory, New York

Appendix: Glossary of terms

Antihole:
Increase in absorption at some frequencies within inhomogeneous line as a result of the hole burning process.

Diagonal energy disorder:
Inhomogeneous broadening caused by glass host or protein environment.

Dispersive kinetics:
Variations in the hole burning rate due to a distribution hole burning rate constant.

Huang–Rhys factor:
A parameter, S, that characterizes the electron-phonon coupling strength. (e^{-S} = Debye–Waller factor).

Homogeneous broadening (Γ_H)*:*
Broadening of the optical transition in chemically identical molecules in identical local environments.

Inhomogeneous broadening (Γ_I)*:*
Additional broadening of an optical line due to distribution of local environments.

Librational motion:
Hindered rotation of coupled molecules in a solid state system.

Marker mode:
Vibrational mode associated with the special pair in a reaction center.

Pseudo-phonon sideband hole (Pseudo PSBH):
Loss of absorption on the low energy side of the laser frequency due to burning of absorbers absorbing at laser frequency via their phonon sideband.

Real phonon sideband hole (Real PSBH):
Loss of absorbers at burn laser frequency leads to decrease in absorption (via phonon sideband) at higher energy than the ZPH.

Spectral diffusion:
Broadening of the absorption line due to fluctuations in glass host on a time scale longer than excited state lifetime.

Zero-phonon hole (ZPH):
Decrease in absorption at the burn laser frequency due to saturation removal of molecules with zero phonon lines at that frequency.

Zero-phonon line (ZPL):
A transition in which no net change of phonons occurs.